Article

Cell Reports

Impaired Expression of Rearranged Immunoglobulin Genes and Premature p53 Activation Block B Cell Development in BMI1 Null Mice

Graphical Abstract

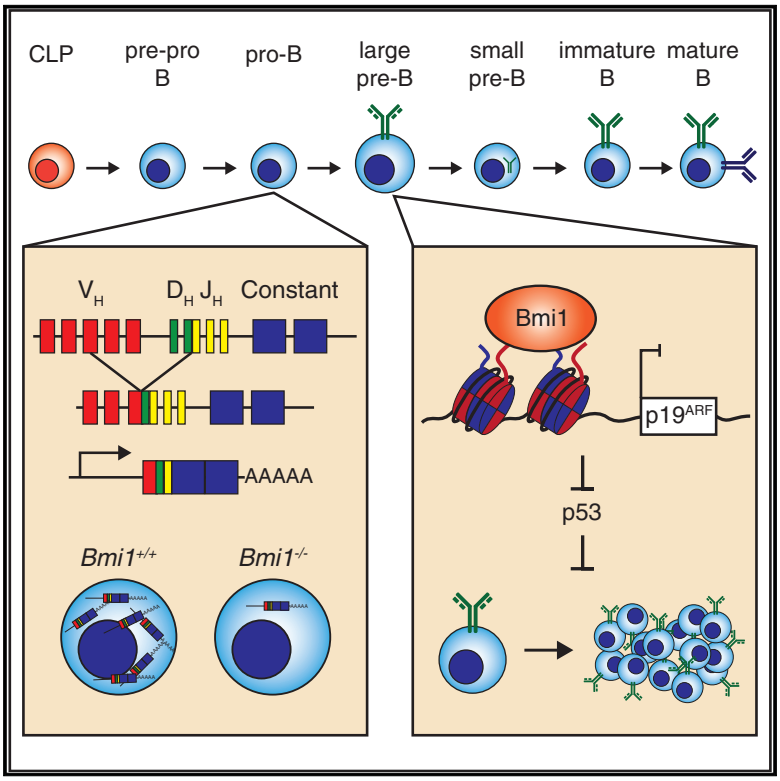

Authors

David J. Cantor, Bryan King, Lili Blumenberg, ..., Sergei B. Koralov, Jane A. Skok, Gregory David

Correspondence

gregory.david@nyumc.org

In Brief

Cantor et al. identify a cell-autonomous role for the polycomb group protein BMI1 in early B cell development. At the pro-B cell to pre-B cell transition, BMI1 promotes the expression of newly rearranged *Igh* genes in pro-B cells and subsequently prevents premature p53 activation and enables large pre-B cell proliferation.

Highlights

- BMI1 is required at the pro-B cell to pre-B cell transition in a cell-autonomous manner
- BMI1 promotes the expression of newly rearranged *Igh* genes in pro-B cells
- BMI1 prevents premature p53 activation and enables large pre-B cell proliferation

Cantor et al., 2019, Cell Reports *26*, 108–118
January 2, 2019
https://doi.org/10.1016/j.celrep.2018.12.030

CellPress

OPEN ACCESS
CellPress

Cell Reports
Article

Impaired Expression of Rearranged Immunoglobulin Genes and Premature p53 Activation Block B Cell Development in BMI1 Null Mice

David J. Cantor,[1] Bryan King,[2,4] Lili Blumenberg,[2] Teresa DiMauro,[1] Iannis Aifantis,[2,4] Sergei B. Koralov,[2] Jane A. Skok,[2,4] and Gregory David[1,3,4,5,*]

[1]Department of Biochemistry and Molecular Pharmacology, New York University School of Medicine, New York, NY 10016, USA
[2]Department of Pathology, New York University School of Medicine, New York, NY 10016, USA
[3]Department of Urology, New York University School of Medicine, New York, NY 10016, USA
[4]Perlmutter Cancer Center, New York University School of Medicine, New York, NY 10016, USA
[5]Lead Contact
*Correspondence: gregory.david@nyumc.org
https://doi.org/10.1016/j.celrep.2018.12.030

SUMMARY

B cell development is a highly regulated process that requires stepwise rearrangement of immunoglobulin genes to generate a functional B cell receptor (BCR). The polycomb group protein BMI1 is required for B cell development, but its function in developing B cells remains poorly defined. We demonstrate that BMI1 functions in a cell-autonomous manner at two stages during early B cell development. First, loss of BMI1 results in a differentiation block at the pro-B cell to pre-B cell transition due to the inability of BMI1-deficient cells to transcribe newly rearranged *Igh* genes. Accordingly, introduction of a pre-rearranged *Igh* allele partially restored B cell development in *Bmi1*$^{-/-}$ mice. In addition, BMI1 is required to prevent premature p53 signaling, and as a consequence, *Bmi1*$^{-/-}$ large pre-B cells fail to properly proliferate. Altogether, our results clarify the role of BMI1 in early B cell development and uncover an unexpected function of BMI1 during VDJ recombination.

INTRODUCTION

B cell development depends on successful gene rearrangements at the immunoglobulin (Ig) loci to ensure that mature B cells express a diverse repertoire of antibodies. During this process, a VDJ_H joint is assembled at the Ig heavy (*Igh*) chain locus in pro-B cells, which, if in the correct reading frame, leads to the expression of an Igμ protein. Igμ assembles with surrogate light chains to form a surface pre-B cell receptor (pre-BCR), which guides the pro-B cell to pre-B cell transition. Following signaling by the pre-BCR, pre-B cells undergo clonal expansion and subsequent rearrangement of the Ig light (*IgL*) chain loci. Successfully rearranged light chains assemble with an Igμ chain, forming a surface BCR, and drive the progression to immature B cells that will form the reservoir of long-lived mature B cells (Herzog et al., 2009).

The process of V(D)J recombination presents inherent risks to the organism because of the generation of double-strand breaks and subsequent non-homologous end joining of DNA fragments at the *Ig* loci. Thus, numerous mechanisms exist to ensure the proper generation of a clonal surface BCR on B cells while preventing deleterious events. These include the sequential rearrangement of *Ig* loci, with several checkpoints along the sequential development to assess rearrangement status, and the programming of developing B cells for either clonal expansion or apoptosis, depending on pre-BCR and BCR signaling cues (Melchers, 2015). While extensive work has elucidated many of these mechanisms, our understanding of the molecular pathways critical for B cell development remains fragmentary.

Polycomb group (PcG) proteins are a group of regulatory factors that form multimeric protein complexes and are critical for maintaining cell identity and cell proliferation by modifying chromatin structure and silencing genes (Sauvageau and Sauvageau, 2010). Polycomb repressive complex 1 (PRC1) and polycomb repressive complex 2 (PRC2) were the earliest complexes described, although more recent work has identified both alternative and novel polycomb complexes. The core components of PRC1 consist of one member of each CBX, HPH, PCGF, and RING1 protein family, which monoubiquitinate histone H2A on lysine 119 (H2AK119), whereas the core components of PRC2 are EED, Suz12, EZH1/2, and RBBP4/7, which methylate H3K27 (Di Croce and Helin, 2013; Simon and Kingston, 2013). PRC1 and PRC2 are thought to cooperate to regulate gene expression, because PRC2 deposition of H3K27me3 recruits PRC1 through its CBX family member (Blackledge et al., 2015). However, inactivation of core PRC2 factors in mammalian cells only partially affects PRC1 recruitment to its target loci and minimally changes global H2AK119ub levels, suggesting that PRC2-independent mechanisms exist for PRC1 recruitment (Tavares et al., 2012).

Through genetic studies in the mouse, it became apparent that PcG proteins are critical for B cell lymphopoiesis. EZH2 regulates distal V_H gene usage during V_H-DJ_H recombination and prevents *IgL* loci rearrangement in pro-B cells (Mandal et al., 2011; Su et al., 2003). The PRC1 component BMI1, also known as PCGF4, is required for normal lymphocyte development at least partly through the repression of the *Ink4*/*Arf* locus, which

encodes the two tumor suppressor proteins, $p16^{INK4A}$ and $p19^{ARF}$ (Bruggeman et al., 2005; Oguro et al., 2010). In developing T cells, BMI1 prevents premature $p19^{ARF}$-mediated stabilization of p53 to promote the proliferation and survival of progenitor T cells in response to pre-T cell receptor (TCR) signaling (Miyazaki et al., 2008). However, *Bmi1*$^{-/-}$ *Ink4a/Arf*$^{-/-}$ mice still exhibit defective B cell lymphopoiesis, suggesting that BMI1 functions partly through *Ink4a/Arf*-independent mechanisms during B cell development (Oguro et al., 2010).

We found that BMI1 is required for pro-B cells to differentiate into pre-B cells in a cell-autonomous manner. Loss of BMI1 results in the upregulation of p53 target genes in pro-B cells, precluding the expansion of these cells at the large pre-B stage. Furthermore, expression of rearranged *Igh* genes and production of the Igμ chain are impaired in *Bmi1*$^{-/-}$ pro-B cells. Accordingly, introduction of a pre-rearranged *Igh* allele partially restored B cell development in *Bmi1*$^{-/-}$ mice. Altogether, these results identify a critical role for BMI1 in B cell development through the regulation of rearranged *Igh* gene expression and expansion of pre-B cells.

RESULTS

BMI1 Is Required for the Pro-B Cell to Pre-B Cell Transition

Previous studies have identified BMI1 as essential for B cell development in the mouse (Oguro et al., 2010; van der Lugt et al., 1994). However, the mechanisms that BMI1 engages to promote B cell development remain unknown. To begin to dissect the function of BMI1 in progenitor B cells, we first assessed its expression levels throughout early B cell development using data acquired through the Immunological Genome Project (Heng et al., 2008; Painter et al., 2011). *Bmi1* is highly expressed in pro-B cells and large pre-B cells and is downregulated as large pre-B cells transition into small pre-B cells (Figure S1A). The expression of *Cdkn2a*, which encodes the tumor suppressor proteins $p16^{INK4A}$ and $p19^{ARF}$ and is repressed by BMI1, inversely correlates with *Bmi1* expression at the pro-B cell to pre-B cell transition (Figure S1A). This correlation disappears in mature B cells, likely pointing to a more critical role for a *Bmi1-Cdkn2a* axis at the pro-B cell to pre-B cell transition. The high expression of *Bmi1* and the resulting repression of *Cdkn2a* early in B cell development are reminiscent of what has been observed in early T cell development, in which BMI1 represses $p19^{ARF}$ to prevent apoptosis in proliferating DN3 T cells (Miyazaki et al., 2008). Furthermore, the inverse correlation of *Bmi1* and *Cdkn2a* levels is consistent with studies demonstrating a modest rescue of B cell development in *Bmi1*$^{-/-}$ *Ink4a/Arf*$^{-/-}$ mice (Miyazaki et al., 2008; Oguro et al., 2010).

To further probe BMI1's function in early B cell development, we determined the frequency and numbers of early B cell progenitors in *Bmi1*$^{+/+}$ and *Bmi1*$^{-/-}$ mice. The bone marrow of *Bmi1*$^{-/-}$ mice was devoid of B cells, correlating with the accumulation of pro-B cells and their failure to differentiate into pre-B cells (Figures 1A and 1B; Figure S1B). The differentiation block at the pro-B cell to pre-B cell transition resulted in drastically fewer mature B cells in the peripheral blood and spleen of *Bmi1*$^{-/-}$ mice and a corresponding increase in the frequency of $CD11b^{+}$ myeloid cells (Figures 1C and 1D). Consistent with previous reports (van der Lugt et al., 1994), we observed a drastic reduction in the cellularity of various hematopoietic organs of *Bmi1*$^{-/-}$ mice as a consequence of the overall reduction in lymphocyte numbers (Figure S1C).

Reduced Igμ Chain Expression in *Bmi1*$^{-/-}$ Pro-B Cells

The pro-B cell to pre-B cell transition and subsequent expansion of large pre-B cells depend on the successful rearrangement of the *Igh* locus, the expression of Igμ chain, the assembly of a pre-BCR on the surface of the cell, and signaling downstream of the pre-BCR. Failure in any of these steps will impair pro-B cell to pre-B cell differentiation (Herzog et al., 2009). We therefore determined whether BMI1 was required for the expression of Igμ chain in pro-B cells. By intracellular flow cytometry analysis, we observed a decrease in the frequency of pro-B cells expressing Igμ chain in *Bmi1*$^{-/-}$ mice to about half of the levels observed in *Bmi1*$^{+/+}$ mice (Figure 2A). In addition, we observed a decrease in the median Igμ fluorescence intensity in Igμ-expressing pro-B cells from *Bmi1*$^{-/-}$ mice (Figure 2B).

BMI1 Is Dispensable for VDJ_H Recombination but Required for Rearranged *Igh* Gene Expression in Pro-B Cells

We next determined the basis for the reduction in Igμ chain expression in *Bmi1*$^{-/-}$ pro-B cells. This reduction could result from inefficient VDJ_H recombination and/or failure to express rearranged *Igh* genes. To assess whether BMI1 inactivation alters VDJ_H recombination, we determined the frequency of rearrangement for two V_H gene families, V_H7183 and V_HJ558, in *Bmi1*$^{+/+}$ and *Bmi1*$^{-/-}$ pro-B cells. The V_H7183 gene family is the most proximal V_H family and the V_HJ558 family is the most distal V_H family to DJ_H genes (Figure S2A). Because the PRC2 component EZH2 is required for distal V_H gene usage (Su et al., 2003), we tested whether BMI1 similarly enabled distal V_H gene usage. On genomic DNA isolated from pro-B cells, we performed semiquantitative PCR using degenerative forward primers that amplify either V_H7183 genes or V_HJ558 genes and a reverse primer specific to the J_H3 gene. *Bmi1*$^{-/-}$ pro-B cells and their wild-type counterparts contained comparable levels of DNA that had recombined either V_H7183 or V_HJ558 genes with DJ_H genes (Figure 2C). In addition, we isolated and sequenced individual VDJ_H joints from *Bmi1*$^{+/+}$ and *Bmi1*$^{-/-}$ pro-B cells using a promiscuous forward primer that amplifies various genes across all V_H families. Again, we observed no difference in the ratio of proximal to distal V_H gene usage between *Bmi1*$^{+/+}$ and *Bmi1*$^{-/-}$ pro-B cells, supporting the conclusion that BMI1 is not required for VDJ_H recombination in pro-B cells (Figure 2D).

In contrast, when we assessed the expression levels of rearranged *Igh* genes, we observed a drastic reduction in the expression levels of all V_H family genes tested in *Bmi1*$^{-/-}$ pro-B cells, consistent with a combined decreased frequency of *Bmi1*$^{-/-}$ pro-B cells expressing Igμ and decreased Igμ protein levels in Igμ-expressing *Bmi1*$^{-/-}$ pro-B cells (Figure 2E). The decrease in rearranged *Igh* gene expression was not the result of a generic reduction in expression at the *Igh* locus, because we detected no difference in the expression of D_H-Cu transcripts (Figure 2E). Altogether, these data support a model in which BMI1 is

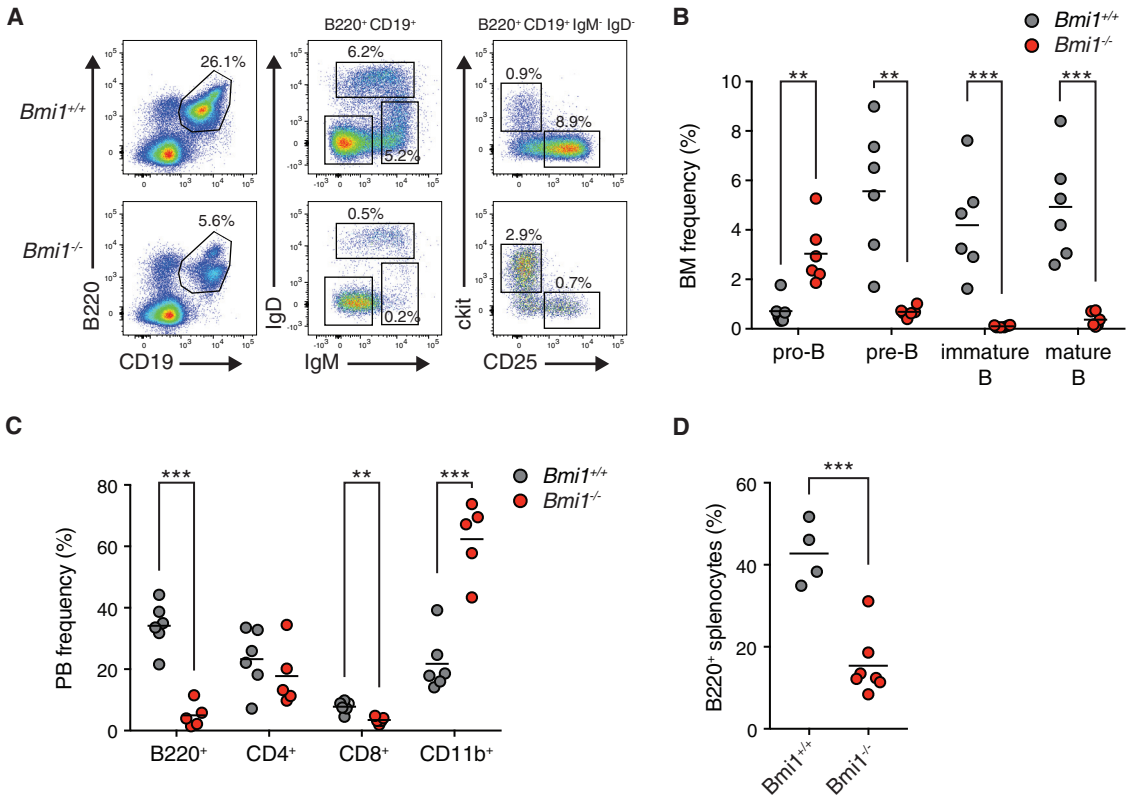

Figure 1. BMI1 Is Required for the Pro-B Cell to Pre-B Cell Transition

(A) Representative fluorescence-activated cell sorting (FACS) plots of developing B cells in the bone marrow of indicated mice. Shown is the frequency of each cell population in the bone marrow of indicated animals. Pro-B: $B220^+$ $CD19^+$ IgM^- IgD^- $ckit^+$ $CD25^-$. Pre-B: $B220^+$ $CD19^+$ IgM^- IgD^- $ckit^+$ $CD25^-$. Immature: $B220^+$ $CD19^+$ IgM^+ IgD^-. Mature: $B220^+$ $CD19^+$ IgM^+ IgD^+.

(B) Frequency of indicated cell populations in the bone marrow of animals. Each point represents one animal; the line represents the mean. n = 6 for each genotype.

(C) Frequency of indicated cell type in the peripheral blood of indicated animals. Each point represents one animal; the line represents the mean. n = 6 for $Bmi1^{+/+}$ animals; n = 5 for $Bmi1^{-/-}$ animals.

(D) Frequency of $B220^+$ cells in the spleens of indicated mice. Each point represents one animal; the line represents the mean. n = 4 for $Bmi1^{+/+}$ animals; n = 7 for $Bmi1^{-/-}$ animals.

***p < 0.001, **p < 0.01. BM, bone marrow; PB, peripheral blood.

See also Figure S1.

dispensable for VDJ_H recombination but is critical for expression of recently rearranged VDJ_H genes in pro-B cells.

BMI1 Is Not Required for *Igh* Germline Transcription or *Igh* Contraction

PRC1 has been shown to regulate high-order chromatin architecture (Simon and Kingston, 2013). For RAG complexes to access V_H genes and initiate recombination, the surrounding chromatin needs to be accessible (Ebert et al., 2013; Fuxa et al., 2004). The transcription of *Igh* genes in germline configuration (germline transcription) has been hypothesized to be critical for RAG accessibility to these genes (Yancopoulos and Alt, 1985). We therefore first assessed whether BMI1 loss altered the ability of the germline *Igh* loci to be transcribed in pro-B cells as a surrogate assay for chromatin accessibility. However, we did not observe differences in germline transcription for either V_H7183 or V_HJ558 gene families between $Bmi1^{+/+}$ and $Bmi1^{-/-}$ pro-B cells (Figure S2B). Because we observed that BMI1 modulates the expression of recombined *Igh* genes in pro-B cells, and given the impact of chromatin architecture on *Igh* recombination (Roldán et al., 2005), we next assessed the impact of BMI1 on high-order organization of the *Igh* loci. With 3D microscopy, we determined whether BMI1 is required for *Igh* contraction by using DNA-fluorescence *in situ* hybridization (FISH) probes against the 5′ *Igh* (distal) and 3′ *Igh* (proximal) regions. Consistent with our finding that $Bmi1^{-/-}$ pro-B cells efficiently use both proximal and distal V_H gene families during V_H-DJ_H joining, the contraction of the *Igh* locus in pro-B cells was not affected by the absence of BMI1 (Figure S2C).

A Pre-rearranged *Igh* Allele Restores B Cell Development in $Bmi1^{-/-}$ Mice

We postulated that if the process of VDJ_H recombination at the *Igh* locus affects the expression of rearranged *Igh* genes in $Bmi1^{-/-}$ pro-B cells and is responsible for the differentiation block of

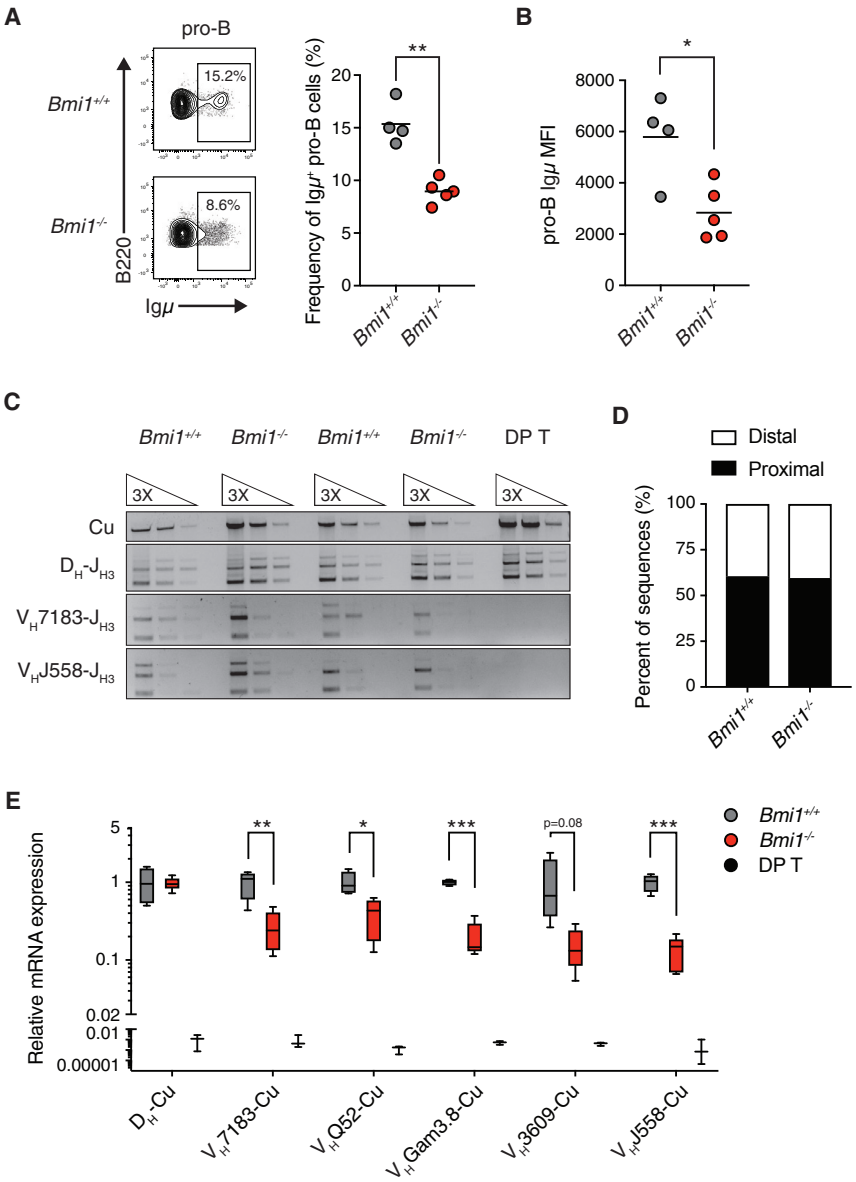

Figure 2. BMI1 Is Required for the Expression of Rearranged *Igh* Genes in Pro-B Cells

(A) Representative FACS plot and quantification of Igμ chain-positive pro-B cells in *Bmi1*$^{+/+}$ and *Bmi1*$^{-/-}$ mice. Each point represents one animal; the line represents the mean. n = 4 for *Bmi1*$^{+/+}$ animals; n = 5 for *Bmi1*$^{-/-}$ animals.

(B) Igμ MFI in Igμ-expressing pro-B cells. Each dot represents one animal; the line represents the mean. n = 4 for *Bmi1*$^{+/+}$ animals; n = 5 for *Bmi1*$^{-/-}$ animals.

(C) Semiquantitative PCR analysis of genomic DNA from sorted *Bmi1*$^{+/+}$ and *Bmi1*$^{-/-}$ pro-B cells assessing the frequency of *Igh* locus rearrangement using either proximal (V_H7183) or distal (V_HJ558) V_H gene segments. DNA from DP T was used as a negative control.

(D) Frequency of proximal and distal V_H segments used in individually sequenced VDJ_H coding joints from sorted pro-B cells. VDJ_H joints were amplified using a promiscuous forward primer (MsVHe) and a reverse primer specific to J_{H3}. n = 37 VDJ_H sequences for *Bmi1*$^{+/+}$ pro-B cells, and n = 48 VDJ_H sequences for *Bmi1*$^{-/-}$ pro-B cells sorted from 3 animals for each genotype.

(E) qRT-PCR analysis of mRNA expression of rearranged *Igh* genes. DP T were used as negative controls. Data are shown as a Tukey box-and-whisker plot; the center line represents the median. n ≥ 5 for each genotype.

***p < 0.001, **p < 0.01, *p < 0.05. MFI, median fluorescence intensity; DP T, double-positive thymocytes.

See also Figure S2.

developing B cells in *Bmi1*$^{-/-}$ mice, the introduction of a pre-rearranged VDJ_H allele would rescue B cell development. To test this, we generated *Bmi1*$^{+/+}$ and *Bmi1*$^{-/-}$ mice carrying a recombined VDJ_H element inserted into the endogenous J_H locus (*B1.8i*) (Sonoda et al., 1997). Consistent with our hypothesis, introduction of the *B1.8i* allele largely restored B cell development to *Bmi1*$^{-/-}$ animals (Figures 3A–3C; Figure S3). The frequencies of immature, mature, and splenic B cells in *Bmi1*$^{-/-}$ *B1.8*$^{+}$ mice were comparable to that of *Bmi1*$^{+/+}$ mice (Figures 3A–3C). Total numbers of *Bmi1*$^{-/-}$ *B1.8*$^{+}$ B cells, while still decreased compared to those of *Bmi1*$^{+/+}$ animals, were drastically increased compared to those of *Bmi1*$^{-/-}$ animals (Figure S3). Moreover, when we assessed Igμ expression in pro-B cells, we found that the *B1.8* allele increased the frequency of *Bmi1*$^{-/-}$ pro-B cells expressing Igμ and restored Igμ protein levels in Igμ-expressing *Bmi1*$^{-/-}$ pro-B cells (Figure 3D).

Altogether, these data demonstrate that bypassing VDJ_H recombination enables *Bmi1*$^{-/-}$ pro-B cells to express Igμ and subsequently differentiate.

BMI1 Loss Results in the Upregulation of p53 Signaling in Pro-B Cells

Although expression of a pre-rearranged *Igh* locus partially rescues B cell development in *Bmi1*$^{-/-}$ mice, *Bmi1*$^{-/-}$ *B1.8i*$^{+}$ bone marrow still contains lower frequencies and numbers of pre-B cells compared to wild-type mice (Figure 3; Figure S3). We therefore sought to identify additional mechanisms engaged by BMI1 that control the pro-B cell to pre-B cell transition in developing B cells. We assessed the expression levels of the B cell transcription factors *Pax5* and *Ebf1*, because BMI1 regulates their expression in early progenitors before lymphoid commitment (Oguro et al., 2010), but we found no difference in their expression between *Bmi1*$^{-/-}$ pro-B cells and their wild-type counterparts (Figure S4A). To uncover other altered pathways, we sorted pro-B cells from *Bmi1*$^{+/+}$ and *Bmi1*$^{-/-}$ mice and performed genome-wide expression analysis. Using a false discovery rate (FDR) < 0.05 as a cutoff for significance, we identified 122 upregulated transcripts and 165 downregulated transcripts in *Bmi1*$^{-/-}$ pro-B cells compared

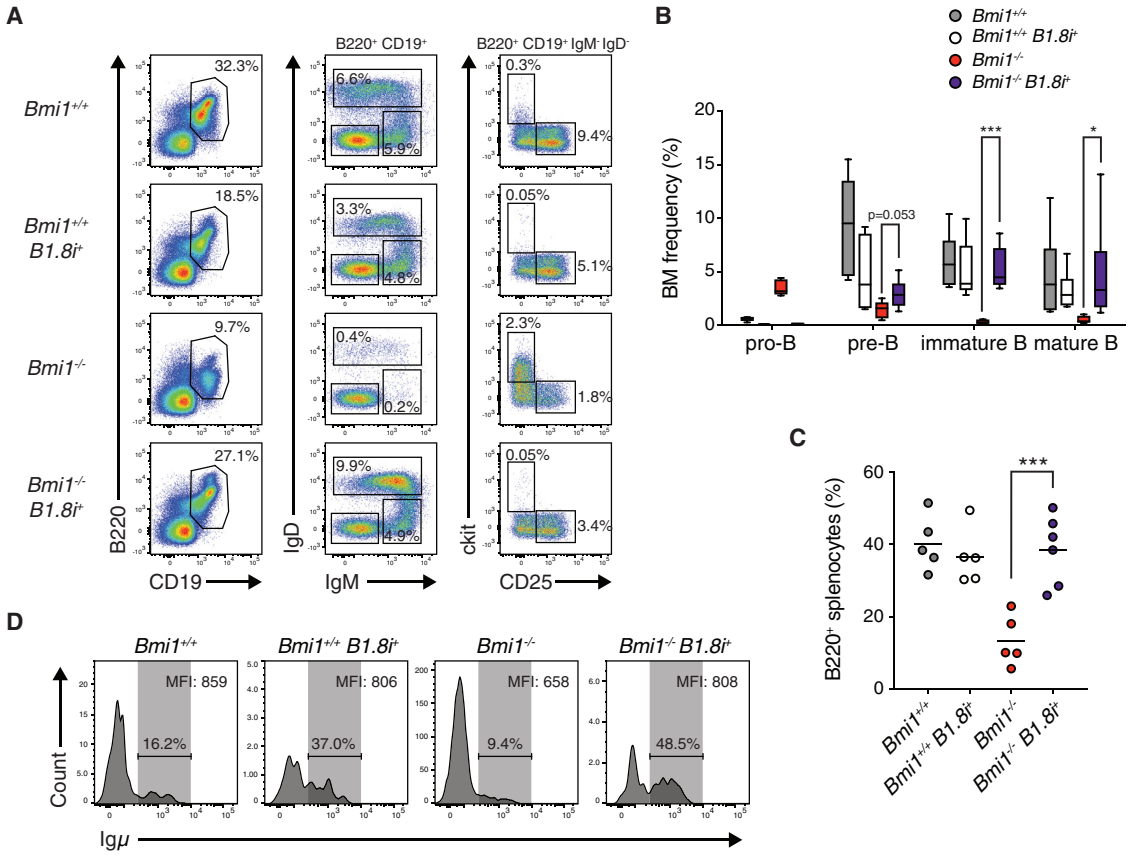

Figure 3. A pre-rearranged *Igh* Locus Restores B Cell Development to *Bmi1*$^{-/-}$ Mice

(A) Representative FACS plot of developing B cells in the bone marrow of indicated mice. Shown is the frequency of each cell population in the bone marrow of indicated animals.

(B) Frequency of indicated cell type in the bone marrow of indicated mice. Data are shown as a Tukey box-and-whisker plot; the center line represents the median. $n \geq 5$ for each genotype.

(C) Frequency of B220^{+} cells in the spleen of indicated mice. Each point represents one animal; the line represents the mean. $n \geq 5$ for each genotype.

(D) Histogram showing the frequency of Igμ-positive pro-B cells from indicated animals. Igμ MFI in Igμ-expressing pro-B cells is indicated in the top right of each plot.

***$p < 0.001$, *$p < 0.05$. BM, bone marrow; MFI, median fluorescence intensity.

See also Figure S3.

to *Bmi1*$^{+/+}$ pro-B cells (Table S1). Numerous p53 targets, including *Bbc3*, *Pmaip1*, *Phlda3*, and *Cdkn1a*, were found among the upregulated transcripts in *Bmi1*$^{-/-}$ pro-B cells (Figure 4A; Table S1). Consistent with this observation, gene ontology analysis of upregulated genes in *Bmi1*$^{-/-}$ pro-B cells showed enrichment for pathways associated with apoptosis, proliferation, DNA damage, and p53 signaling (Figure S4B). Similarly, the p53 pathway was enriched in *Bmi1*$^{-/-}$ pro-B cells when analyzed by gene set enrichment analysis (GSEA) (Figure S4C). As expected, *p19*^{Arf} expression was drastically upregulated in *Bmi1*$^{-/-}$ pro-B cells, demonstrating de-repression of the *Ink4a/Arf* locus, and we confirmed the upregulation of specific p53 target genes, including *Bbc3*, *Pmaip1*, *Phlda3*, and *Cdkn1a*, in *Bmi1*$^{-/-}$ pro-B cells from independent animals (Figure 4B). We did not detect changes in *Trp53* transcript levels, suggesting BMI1-dependent post-transcriptional regulation of p53 activity (Figure 4B). Together with previous work demonstrating that deletion of *p19*^{Arf} partially restores B cell development to *Bmi1*$^{-/-}$ mice (Akala et al., 2008; Miyazaki et al., 2008; Oguro et al., 2006) and our analysis of the expression of *Bmi1* and *Ckdn2a* in progenitor B cells (Figure S1A), these findings are consistent with a role for BMI1 in preventing p53 signaling through the repression of the *Ink4a/Arf* locus in developing pro-B cells.

p53 signaling generally results in either apoptosis or cell-cycle arrest (Kruse and Gu, 2009). In progenitor T cells, BMI1 prevents apoptosis through the inhibition of the p19^{ARF}-p53 pathway (Miyazaki et al., 2008). Therefore, we first tested whether increased apoptosis was occurring in developing *Bmi1*$^{-/-}$ B cells. However, we did not observe differences in the frequency of annexin V-positive pro-B cells or pre-B cells in *Bmi1*$^{-/-}$ mice compared to wild-type counterparts (Figure 4C). Following successful VDJ$_H$ recombination, signaling through the pre-BCR provides survival cues and promotes the proliferation of large pre-B

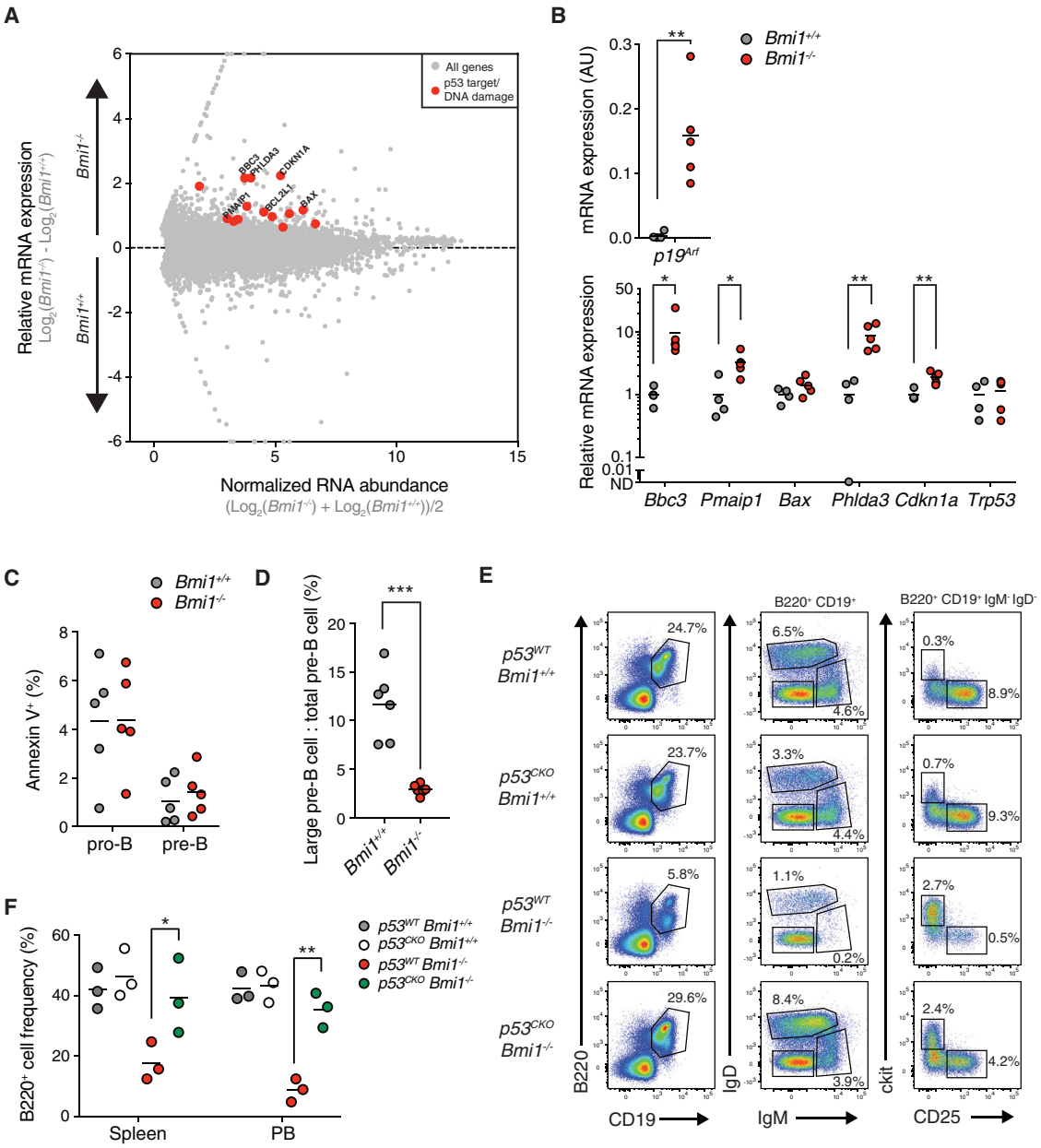

Figure 4. BMI1 Prevents the Upregulation of p53 Signaling and Maintains Large Pre-B Cell Cycling

(A) RNA sequencing (RNA-seq) MA (log ratio and mean average) plot of *Bmi1*$^{+/+}$ versus *Bmi1*$^{-/-}$ pro-B cells. Known targets of p53 are depicted in red.

(B) qRT-PCR expression analysis of indicated genes from sorted pro-B cells of indicated mice. Each point represents one animal; the line represents the mean. n = 4 for *Bmi1*$^{+/+}$ animals; n = 5 for *Bmi1*$^{-/-}$ animals.

(C) Frequency of apoptotic (as indicated by annexin V positivity) pro-B cells and pre-B cells of indicated mice. Each point represents one animal; the line represents the mean. n = 5 for each genotype.

(D) Frequency of large pre-B cells present in the pre-B cell compartment of indicated mice. Each point represents one animal; the line represents the mean. n = 6 for each genotype.

(E) FACS plot of developing B cells in the bone marrow of indicated mice. Shown is the frequency of each cell population in the bone marrow of indicated animals. Representative of 3 independent experiments.

(F) Frequency of B220^{+} cells in the spleen and peripheral blood of indicated mice. Each point represents one animal; the line represents the mean. n = 3 for each genotype.

***p < 0.001, **p < 0.01, *p < 0.05. PB, peripheral blood.

See also Figure S4 and Table S1.

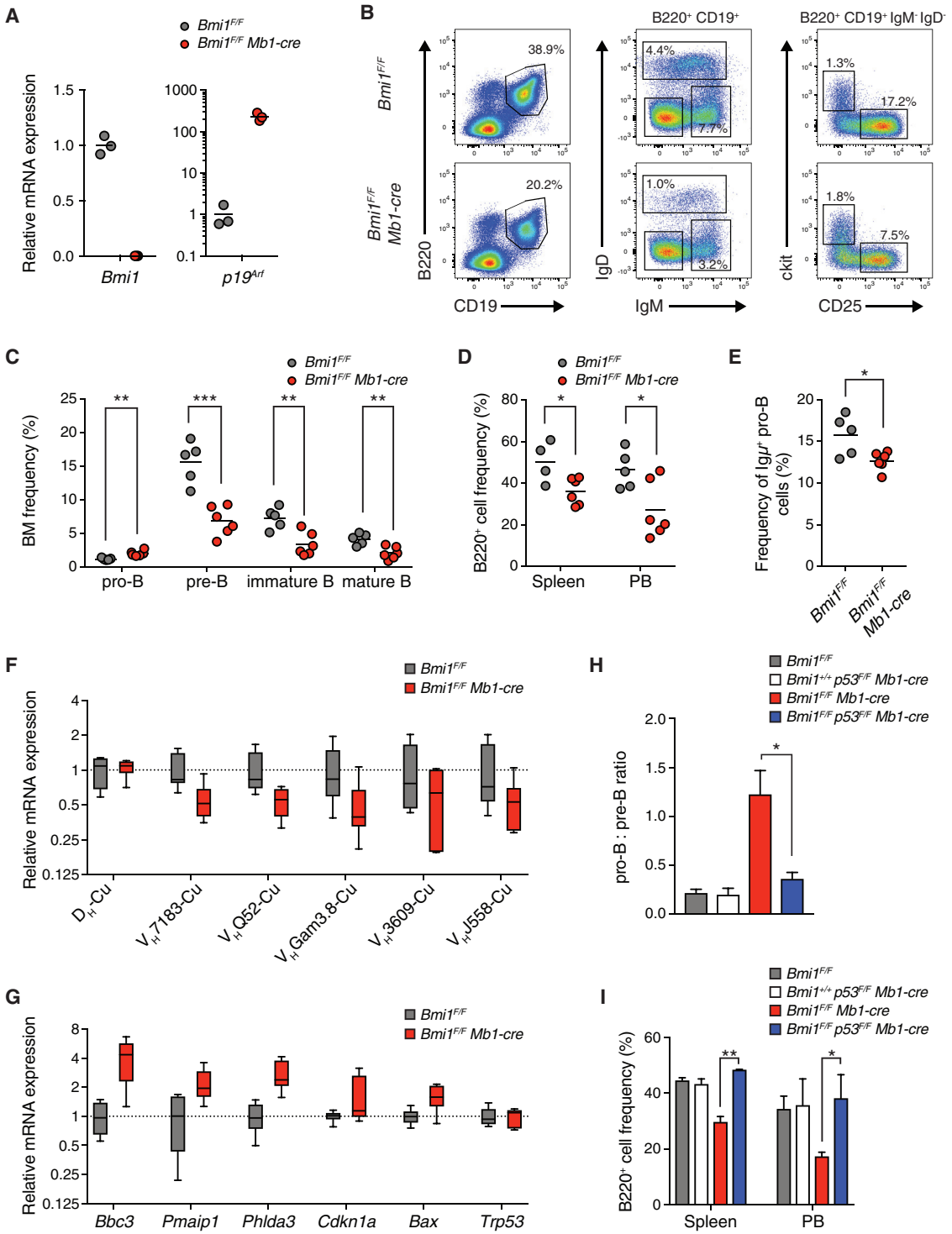

Figure 5. BMI1 Regulates the Pro-B Cell to Pre-B Cell Transition in a Cell-Autonomous Manner

(A) mRNA expression levels as determined by qRT-PCR of indicated genes from pro-B cells of indicated mice. Each point represents one animal; the line represents the mean. n = 3 for each genotype.

(B) Representative FACS plot of developing B cells in the bone marrow of indicated mice. Shown is the frequency of each cell population in the bone marrow of indicated animals.

(C) Frequency of developing B cells in the bone marrow of indicated mice. Each point represents one animal; the line represents the mean. n = 5 for *Bmi1*$^{F/F}$ animals; n = 6 for *Bmi1*$^{F/F}$ *Mb1-cre* animals.

(legend continued on next page)

cells. Following this proliferative burst, pre-B cells become quiescent, differentiate into small pre-B cells, and subsequently rearrange their *IgL* loci (Herzog et al., 2009). Therefore, we assessed whether the increased p53 signaling prevented the capacity of *Bmi1*$^{-/-}$ large pre-B cells to clonally expand. Large and small pre-B cells can be distinguished by gating on forward scatter within the pre-B cell population. Using this strategy, we observed that *Bmi1*$^{-/-}$ mice have a drastically lower proportion of large pre-B cells in their pre-B cell compartment (Figure 4D). Moreover, the frequency of proliferating cells, as assessed either by DNA content or by bromodeoxyuridine (BrdU) incorporation, in the pre-B cell compartment was decreased in *Bmi1*$^{-/-}$ animals (Figures S4D and S4E). We subsequently hypothesized that *Bmi1*$^{-/-}$ *B1.8*$^{+}$ mice may still exhibit decreased pre-B cells numbers (Figure 3; Figure S3) due to their inability to clonally expand. Consistent with this hypothesis, there was a comparable reduction both in the proportion of large pre-B cells in the pre-B cell compartment and in the frequency of BrdU-positive pre-B cells between *Bmi1*$^{-/-}$ mice and *Bmi1*$^{-/-}$ *B1.8*$^{+}$ mice (Figures S4F and S4G).

Finally, to demonstrate that BMI1 functions upstream of p53 to prevent B cell development, we generated a cohort of animals (*p53*$^{F/F}$ *Bmi1*$^{+/+}$, *p53*$^{F/F}$ *Bmi1*$^{+/+}$ *Mx1-cre*, *p53*$^{F/F}$ *Bmi1*$^{-/-}$, and *p53*$^{F/F}$ *Bmi1*$^{-/-}$ *Mx1-cre*, hereafter referred to as *p53*^{WT} *Bmi1*$^{+/+}$, *p53*^{CKO} *Bmi1*$^{+/+}$, *p53*^{WT} *Bmi1*$^{-/-}$, and *p53*^{CKO} *Bmi1*$^{-/-}$), in which p53 was acutely deleted following serial injections of poly(I:C). We found that acute p53 deletion partially restored the pro-B cell to pre-B cell transition and the frequency of mature B cells in the periphery in *Bmi1*$^{-/-}$ mice (Figures 4E and 4F). Altogether, these data demonstrate that aberrant p53 signaling caused by BMI1 loss prevents the clonal expansion of large pre-B cells.

BMI1 Is Required for the Pro-B Cell to Pre-B Cell Transition in a Cell-Autonomous Manner

It has previously been postulated that the microenvironment of *Bmi1*$^{-/-}$ mice is defective in supporting B cell lymphopoiesis (Oguro et al., 2010). To test whether the defects observed in *Bmi1*$^{-/-}$ mice reflected non-cell-autonomous effects of BMI1 on developing B cells, we generated animals in which *Bmi1* is deleted selectively in pro-B cells and their progeny, using the *Mb1-cre* transgene (Hobeika et al., 2006). We confirmed efficient deletion of *Bmi1* and the resulting increased expression of the BMI1-target gene *p19*^{Arf} in pro-B cells sorted from *Bmi1*$^{F/F}$ *Mb1-cre* mice (Figure 5A). *Bmi1*$^{F/F}$ *Mb1-cre* mice presented with reduced total cell numbers in their bone marrow, spleen, and peripheral blood and a roughly 2-fold reduction in the frequency of B cells in the bone marrow (Figures S5A and S5B). Consistent with our observations in *Bmi1*$^{-/-}$ mice, cell-autonomous BMI1 loss impaired the pro-B cell to pre-B cell transition, as evidenced by the increased frequency of pro-B cells and the decreased frequency of pre-B cells, in the bone marrow of *Bmi1*$^{F/F}$ *Mb1-cre* mice (Figures 5B and 5C). In addition, we observed a reduction in the frequency of B cells in the peripheral tissues of *Bmi1*$^{F/F}$ *Mb1-cre* mice (Figure 5D). The fraction of pro-B cells expressing intracellular Igμ chain was reduced in *Bmi1*$^{F/F}$ *Mb1-cre* mice (Figure 5E), consistent with the decreased expression of rearranged *Igh* genes (Figure 5F). Again, we observed no difference in the expression of *Pax5* or *Ebf1* in *Bmi1*$^{F/F}$ *Mb1-cre* pro-B cells (Figure S5C), but we did observe higher levels of p53 target genes (Figure 5G). Finally, subsequent deletion of p53 alleviated the pro-B cell to pre-B cell differentiation block and largely restored the frequency of mature B cells in the periphery to *Bmi1*$^{F/F}$ *Mb1-cre* mice (Figures 5H and 5I; Figure S5D). Altogether, these data demonstrate that the defects in B cell differentiation observed in *Bmi1*$^{-/-}$ mice are largely recapitulated by cell-autonomous loss of BMI1.

DISCUSSION

Prior studies have shown that BMI1 is critical for developing lymphocytes; however, the molecular pathways BMI1 engages to promote B cell development have remained poorly defined, and whether the role of BMI1 in B cell development was cell intrinsic remained to be elucidated (Akala et al., 2008; Oguro et al., 2010; van der Lugt et al., 1994). Our analysis identified a cell-autonomous role for BMI1 at two stages during early B cell development. Specifically, BMI1 promotes the expression of rearranged *Igh* genes in pro-B cells and enables large pre-B cell proliferation following pre-BCR signaling through its inhibition of p53 signaling.

In adult stem cells, PRC1 directly binds to and compacts the *Ink4a/Arf* locus, thus repressing the expression of the cell-cycle inhibitors p16^{INK4A} and p19^{ARF} and maintaining stem cell self-renewal capacity (Jacobs et al., 1999; Lessard and Sauvageau, 2003; Molofsky et al., 2003; Park et al., 2003). In BMI1 null mice, the failure to develop mature lymphocytes is due to increased expression of p19^{ARF}, but not increased expression of p16^{INK4A}, as demonstrated by genetic studies in mice (Akala et al., 2008). In support of this observation, loss of BMI1 in developing thymocytes results in the upregulation of p19^{ARF} and the premature stabilization of p53, preventing DN3 T cell proliferation downstream of pre-TCR signaling (Miyazaki et al., 2008).

(D) Frequency of B220^{+} cells in the spleen and peripheral blood of indicated mice. Each point represents one animal; the line represents the mean. n = 4 for *Bmi1*$^{F/F}$ animals; n = 6 for *Bmi1*$^{F/F}$ *Mb1-cre* animals.

(E) Frequency of Igμ-positive pro-B cells in indicated mice. Each point represents one animal; the line represents the mean. n = 5 for *Bmi1*$^{F/F}$ animals; n = 6 for *Bmi1*$^{F/F}$ *Mb1-cre* animals.

(F) qRT-PCR analysis of gene expression of rearranged *Igh* genes in indicated mice. Data are shown as a box-and-whisker plot, with whiskers showing minimum and maximum values; the center line represents the median. n = 6 for each genotype.

(G) qRT-PCR expression analysis of indicated genes from sorted pro-B cells from indicated mice. Data are shown as a box-and-whisker plot, with whiskers showing minimum and maximum values; the center line represents the median. n = 6 for each genotype.

(H) Ratio of the frequency of pro-B cells to pre-B cells in the bone marrow of indicated mice. Data represent mean ± SEM; n = 3 for each genotype.

(I) Frequency of B220^{+} cells in the spleen and peripheral blood of indicated mice. Data represent mean ± SEM; n = 3 for each genotype.

**p < 0.01, *p < 0.05. BM, bone marrow; PB, peripheral blood.

See also Figure S5.

In agreement with these studies, we found that in developing B cells, the expression level of *Bmi1* is high in proliferating pro-B cells and large pre-B cells and subsequently downregulated in quiescent small pre-B cells and immature B cells. Moreover, loss of BMI1 resulted in the increased expression of p53 target genes in pro-B cells and prevented large pre-B cell expansion following pre-BCR signaling. Our data indicating that genetic inactivation of p53 restored B cell development in $Bmi1^{-/-}$ mice, with previous studies showing a partial rescue of peripheral B cells in $Bmi1^{-/-}$ $p19^{Arf-/-}$ double-knockout mice, support a model whereby BMI1 repression of $p19^{Arf}$ is critical to prevent the stabilization of p53 and premature cell-cycle withdrawal of cycling pre-B lymphocytes.

Past studies had demonstrated that genetic inaction of the *Ink4a/Arf* locus only partially restores B cell development to BMI1 null mice (Oguro et al., 2010). These observations suggested that BMI1 functioned through unknown *Ink4a/Arf*-independent mechanisms to promote B cell development. It was initially postulated that this may be through non-cell-autonomous pathways, because transplantation studies suggested the bone marrow of $Bmi1^{-/-}$ mice was defective at supporting B cell development (Oguro et al., 2010). We found that in $Bmi1^{-/-}$ mice, developing B cells fail to progress through the pro-B cell to pre-B cell transition due to the failure of pro-B cells to express rearranged *Igh* genes. Accordingly, the introduction of a pre-rearranged *Igh* locus largely restored B cell development to BMI1 null mice. The pre-rearranged *Igh* allele did not restore the ability of $Bmi1^{-/-}$ large pre-B cells to clonally expand, highlighting the two distinct roles BMI1 plays during early B cell development. Finally, we recapitulated the B cell defects observed in $Bmi1^{-/-}$ mice using a pro-B cell-specific Cre transgene, indicating that cell-autonomous mechanisms of BMI1 in progenitor B cells are sufficient to explain the B cell phenotypes observed in BMI1 null mice.

The exact mechanism BMI1 engages to promote the expression of rearranged *Igh* genes remains unclear. The identification that PRC1 is recruited to sites of double-strand breaks (DSBs) and is required for their efficient repair *in vitro* suggests that a similar process may occur during VDJ_H recombination (Facchino et al., 2010; Ginjala et al., 2011; Ismail et al., 2010). Moreover, BMI1 associates with and recruits factors known to be critical for repair of VDJ_H joints, such as ATM, KU70, and 53BP1, to sites of DSBs (Facchino et al., 2010; Pan et al., 2011; Ui et al., 2015). However, our data demonstrate that BMI1 is not required for VDJ_Hrecombination. In addition, we did not observe an increased frequency of γH2A.X foci at the *Igh* locus in $Bmi1^{-/-}$ pro-B cells (data not shown). These differences may stem from the fact that BMI1 is not absolutley required but instead increases the efficiency of DSB resolution, coupled with the higher-sensitivity assays used to detect DSBs in the absence of BMI1 *in vitro* (Facchino et al., 2010; Ismail et al., 2010; Pan et al., 2011). Alternatively, BMI1 may function downstream of DSB repair to enable to expression of recently damaged loci. Immediately following the generation of DSBs, BMI1 is required to prevent premature transcription of damaged genes through the deposition of H2AK119ub and the inhibition of both the FACT (facilitates chromatin transcription) histone chaperone complex and RNA polymerase II elongation (Sanchez et al., 2016; Ui et al., 2015). In the wake of this temporal transcriptional silencing, new uniquely marked histones, such as H3.3, are deposited. The deposition of H3.3 primes recently damaged chromatin and is required for transcription restart (Adam et al., 2013). Another study demonstrated that FACT-mediated histone exchange was required for transcription restart following UV damage (Dinant et al., 2013). However, no studies have demonstrated what happens to transcription restart at sites of DSBs if the initial transcriptional repression does not occur. It is therefore possible that BMI1-dependent transcriptional silencing following the generation of DSBs is required to permit the proper turnover of histones and subsequent re-expression of repaired genes, in this case the recently rearranged *Igh* genes.

BMI1 is overexpressed in several hematologic malignancies, and its upregulation predicts poor prognosis in pediatric B cell acute lymphoblastic leukemia (B-ALL), the most common cancer in children (Peng et al., 2017; Sahasrabuddhe, 2016). Work has shown that pre-BCR and downstream signaling promote the aggressiveness of certain subtypes of B-ALL and can be targeted to eliminate human and mouse B-ALL cells (Eswaran et al., 2015; Feldhahn et al., 2005; Geng et al., 2015; Rickert, 2013). It is therefore tempting to speculate that increased BMI1 expression promotes the inappropriate proliferation of B-ALL cells downstream of pre-BCR signaling in a process analogous to what we observed in normal developing B cells. If so, BMI1-dependent signaling might present a novel therapeutic approach to target B-ALL cell growth. Along these lines, a chemical inhibitor specific to BMI1 was identified and well tolerated in mice (Kreso et al., 2014). Moreover, the inhibitor has been shown to be effective in various cancer cells (Kreso et al., 2014; Yong et al., 2016).

Our study clarifies the function of BMI1 in early B cell development, revealing a critical role for BMI1 for the expression of rearranged *Igh* genes in pro-B cells and the clonal expansion of large pre-B cells, and adds to the expanding range of BMI1's function *in vivo*.

STAR★METHODS

Detailed methods are provided in the online version of this paper and include the following:

- KEY RESOURCES TABLE
- CONTACT FOR REAGENT AND RESOURCE SHARING
- EXPERIMENTAL MODEL AND SUBJECT DETAILS
- METHOD DETAILS
  - Mouse treatment
  - Flow cytometry analysis and cell sorting
  - RNA-sequencing
  - Cell cycle analysis
  - RT-qPCR analysis
  - Semiquantitative PCR analysis of VDJ_H joints
  - Sub-clonal sequencing of VDJ_H joints
  - DNA FISH
  - Confocal microscopy and analysis
- QUANTIFICATION AND STATISTICAL ANALYSIS
- DATA AND SOFTWARE AVAILABILITY

SUPPLEMENTAL INFORMATION

Supplemental Information includes five figures and four tables and can be found with this article online at https://doi.org/10.1016/j.celrep.2018.12.030.

ACKNOWLEDGMENTS

We are grateful to all members of the David laboratory for helpful discussions during the preparation of the manuscript. We wish to acknowledge the Skirball Institute of Biomolecular Medicine for hosting our laboratory following Hurricane Sandy. We thank the NYU Cytometry and Cell Sorting Core (supported in part by NIH/NCI support grant P30CA016087) for help with analysis and cell sorting. We thank the NYU Genome Technology Center (supported in part by NIH/NCI support grant P30CA016087) for help with RNA sequencing and bioinformatic analysis. This work was funded by the NIH (R01CA148639, R21CA155736, and R21CA206013 to G.D.), the Samuel Waxman Cancer Research Foundation (to G.D.), and a Feinberg NYU individual grant (to G.D.). D.J.C. was supported by a NIH MSTP training grant (T32GM007308), a predoctoral NIH/NCI training grant (T32CA009161), and a predoctoral NIH/NCI NRSA (F30CA203047).

AUTHOR CONTRIBUTIONS

D.J.C. performed and designed experiments, analyzed the data, and wrote the manuscript. B.K., L.B., and T.D. performed experiments and contributed to the analysis of the data. I.A., S.B.K., and J.A.S. designed experiments, supplied reagents, and provided scientific input. G.D. oversaw the project, designed experiments, analyzed data, and wrote the manuscript. All authors participated in preparation of the manuscript.

DECLARATION OF INTERESTS

The authors declare no competing interests.

Received: September 7, 2018
Revised: November 1, 2018
Accepted: December 5, 2018
Published: January 2, 2019

REFERENCES

Adam, S., Polo, S.E., and Almouzni, G. (2013). Transcription recovery after DNA damage requires chromatin priming by the H3.3 histone chaperone HIRA. Cell *155*, 94–106.

Akala, O.O., Park, I.-K., Qian, D., Pihalja, M., Becker, M.W., and Clarke, M.F. (2008). Long-term haematopoietic reconstitution by Trp53−/−p16Ink4a−/− p19Arf−/− multipotent progenitors. Nature *453*, 228–232.

Blackledge, N.P., Rose, N.R., and Klose, R.J. (2015). Targeting Polycomb systems to regulate gene expression: modifications to a complex story. Nat. Rev. Mol. Cell Biol. *16*, 643–649.

Bruggeman, S.W., Valk-Lingbeek, M.E., van der Stoop, P.P., Jacobs, J.J., Kieboom, K., Tanger, E., Hulsman, D., Leung, C., Arsenijevic, Y., Marino, S., and van Lohuizen, M. (2005). Ink4a and Arf differentially affect cell proliferation and neural stem cell self-renewal in Bmi1-deficient mice. Genes Dev. *19*, 1438–1443.

Chaumeil, J., Augui, S., Chow, J.C., and Heard, E. (2008). Combined immunofluorescence, RNA fluorescent in situ hybridization, and DNA fluorescent in situ hybridization to study chromatin changes, transcriptional activity, nuclear organization, and X-chromosome inactivation. Methods Mol. Biol. *463*, 297–308.

Di Croce, L., and Helin, K. (2013). Transcriptional regulation by Polycomb group proteins. Nat. Struct. Mol. Biol. *20*, 1147–1155.

Dinant, C., Ampatziadis-Michailidis, G., Lans, H., Tresini, M., Lagarou, A., Grosbart, M., Theil, A.F., van Cappellen, W.A., Kimura, H., Bartek, J., et al. (2013). Enhanced chromatin dynamics by FACT promotes transcriptional restart after UV-induced DNA damage. Mol. Cell *51*, 469–479.

Ebert, A., Medvedovic, J., Tagoh, H., Schwickert, T.A., and Busslinger, M. (2013). Control of antigen receptor diversity through spatial regulation of V(D)J recombination. Cold Spring Harb. Symp. Quant. Biol. *78*, 11–21.

Eswaran, J., Sinclair, P., Heidenreich, O., Irving, J., Russell, L.J., Hall, A., Calado, D.P., Harrison, C.J., and Vormoor, J. (2015). The pre-B-cell receptor checkpoint in acute lymphoblastic leukaemia. Leukemia *29*, 1623–1631.

Facchino, S., Abdouh, M., Chatoo, W., and Bernier, G. (2010). BMI1 confers radioresistance to normal and cancerous neural stem cells through recruitment of the DNA damage response machinery. J. Neurosci. *30*, 10096–10111.

Feldhahn, N., Klein, F., Mooster, J.L., Hadweh, P., Sprangers, M., Wartenberg, M., Bekhite, M.M., Hofmann, W.K., Herzog, S., Jumaa, H., et al. (2005). Mimicry of a constitutively active pre-B cell receptor in acute lymphoblastic leukemia cells. J. Exp. Med. *201*, 1837–1852.

Fuxa, M., Skok, J., Souabni, A., Salvagiotto, G., Roldan, E., and Busslinger, M. (2004). Pax5 induces V-to-DJ rearrangements and locus contraction of the immunoglobulin heavy-chain gene. Genes Dev. *18*, 411–422.

Geng, H., Hurtz, C., Lenz, K.B., Chen, Z., Baumjohann, D., Thompson, S., Goloviznina, N.A., Chen, W.Y., Huan, J., LaTocha, D., et al. (2015). Self-enforcing feedback activation between BCL6 and pre-B cell receptor signaling defines a distinct subtype of acute lymphoblastic leukemia. Cancer Cell *27*, 409–425.

Ginjala, V., Nacerddine, K., Kulkarni, A., Oza, J., Hill, S.J., Yao, M., Citterio, E., van Lohuizen, M., and Ganesan, S. (2011). BMI1 is recruited to DNA breaks and contributes to DNA damage-induced H2A ubiquitination and repair. Mol. Cell. Biol. *31*, 1972–1982.

Heng, T.S., and Painter, M.W.; Immunological Genome Project Consortium (2008). The Immunological Genome Project: networks of gene expression in immune cells. Nat. Immunol. *9*, 1091–1094.

Herzog, S., Reth, M., and Jumaa, H. (2009). Regulation of B-cell proliferation and differentiation by pre-B-cell receptor signalling. Nat. Rev. Immunol. *9*, 195–205.

Hobeika, E., Thiemann, S., Storch, B., Jumaa, H., Nielsen, P.J., Pelanda, R., and Reth, M. (2006). Testing gene function early in the B cell lineage in mb1-cre mice. Proc. Natl. Acad. Sci. USA *103*, 13789–13794.

Ismail, I.H., Andrin, C., McDonald, D., and Hendzel, M.J. (2010). BMI1-mediated histone ubiquitylation promotes DNA double-strand break repair. J. Cell Biol. *191*, 45–60.

Jacobs, J.J.L., Kieboom, K., Marino, S., DePinho, R.A., and van Lohuizen, M. (1999). The oncogene and Polycomb-group gene bmi-1 regulates cell proliferation and senescence through the ink4a locus. Nature *397*, 164–168.

Kreso, A., van Galen, P., Pedley, N.M., Lima-Fernandes, E., Frelin, C., Davis, T., Cao, L., Baiazitov, R., Du, W., Sydorenko, N., et al. (2014). Self-renewal as a therapeutic target in human colorectal cancer. Nat. Med. *20*, 29–36.

Kruse, J.P., and Gu, W. (2009). Modes of p53 regulation. Cell *137*, 609–622.

Kühn, R., Schwenk, F., Aguet, M., and Rajewsky, K. (1995). Inducible gene targeting in mice. Science *269*, 1427–1429.

Lessard, J., and Sauvageau, G. (2003). Bmi-1 determines the proliferative capacity of normal and leukaemic stem cells. Nature *423*, 255–260.

Mandal, M., Powers, S.E., Maienschein-Cline, M., Bartom, E.T., Hamel, K.M., Kee, B.L., Dinner, A.R., and Clark, M.R. (2011). Epigenetic repression of the Igk locus by STAT5-mediated recruitment of the histone methyltransferase Ezh2. Nat. Immunol. *12*, 1212–1220.

Marino, S., Vooijs, M., van Der Gulden, H., Jonkers, J., and Berns, A. (2000). Induction of medulloblastomas in p53-null mutant mice by somatic inactivation of Rb in the external granular layer cells of the cerebellum. Genes Dev. *14*, 994–1004.

Maynard, M.A., Ferretti, R., Hilgendorf, K.I., Perret, C., Whyte, P., and Lees, J.A. (2014). Bmi1 is required for tumorigenesis in a mouse model of intestinal cancer. Oncogene *33*, 3742–3747.

Melchers, F. (2015). Checkpoints that control B cell development. J. Clin. Invest. *125*, 2203–2210.

Miyazaki, M., Miyazaki, K., Itoi, M., Katoh, Y., Guo, Y., Kanno, R., Katoh-Fukui, Y., Honda, H., Amagai, T., van Lohuizen, M., et al. (2008). Thymocyte proliferation induced by pre-T cell receptor signaling is maintained through polycomb gene product Bmi-1-mediated Cdkn2a repression. Immunity *28*, 231–245.

Molofsky, A.V., Pardal, R., Iwashita, T., Park, I.K., Clarke, M.F., and Morrison, S.J. (2003). Bmi-1 dependence distinguishes neural stem cell self-renewal from progenitor proliferation. Nature *425*, 962–967.

Oguro, H., Iwama, A., Morita, Y., Kamijo, T., van Lohuizen, M., and Nakauchi, H. (2006). Differential impact of Ink4a and Arf on hematopoietic stem cells and their bone marrow microenvironment in Bmi1-deficient mice. J. Exp. Med. *203*, 2247–2253.

Oguro, H., Yuan, J., Ichikawa, H., Ikawa, T., Yamazaki, S., Kawamoto, H., Nakauchi, H., and Iwama, A. (2010). Poised lineage specification in multipotential hematopoietic stem and progenitor cells by the polycomb protein Bmi1. Cell Stem Cell *6*, 279–286.

Painter, M.W., Davis, S., Hardy, R.R., Mathis, D., and Benoist, C.; Immunological Genome Project Consortium (2011). Transcriptomes of the B and T lineages compared by multiplatform microarray profiling. J. Immunol. *186*, 3047–3057.

Pan, M.R., Peng, G., Hung, W.C., and Lin, S.Y. (2011). Monoubiquitination of H2AX protein regulates DNA damage response signaling. J. Biol. Chem. *286*, 28599–28607.

Park, I.K., Qian, D., Kiel, M., Becker, M.W., Pihalja, M., Weissman, I.L., Morrison, S.J., and Clarke, M.F. (2003). Bmi-1 is required for maintenance of adult self-renewing haematopoietic stem cells. Nature *423*, 302–305.

Peng, H.X., Liu, X.D., Luo, Z.Y., Zhang, X.H., Luo, X.Q., Chen, X., Jiang, H., and Xu, L. (2017). Upregulation of the proto-oncogene Bmi-1 predicts a poor prognosis in pediatric acute lymphoblastic leukemia. BMC Cancer *17*, 76.

Rickert, R.C. (2013). New insights into pre-BCR and BCR signalling with relevance to B cell malignancies. Nat. Rev. Immunol. *13*, 578–591.

Roldán, E., Fuxa, M., Chong, W., Martinez, D., Novatchkova, M., Busslinger, M., and Skok, J.A. (2005). Locus 'decontraction' and centromeric recruitment contribute to allelic exclusion of the immunoglobulin heavy-chain gene. Nat. Immunol. *6*, 31–41.

Sahasrabuddhe, A.A. (2016). BMI1: a biomarker of hematologic malignancies. Biomark. Cancer *8*, 65–75.

Sanchez, A., De Vivo, A., Uprety, N., Kim, J., Stevens, S.M., Jr., and Kee, Y. (2016). BMI1-UBR5 axis regulates transcriptional repression at damaged chromatin. Proc. Natl. Acad. Sci. USA *113*, 11243–11248.

Sauvageau, M., and Sauvageau, G. (2010). Polycomb group proteins: multi-faceted regulators of somatic stem cells and cancer. Cell Stem Cell *7*, 299–313.

Simon, J.A., and Kingston, R.E. (2013). Occupying chromatin: Polycomb mechanisms for getting to genomic targets, stopping transcriptional traffic, and staying put. Mol. Cell *49*, 808–824.

Sonoda, E., Pewzner-Jung, Y., Schwers, S., Taki, S., Jung, S., Eilat, D., and Rajewsky, K. (1997). B cell development under the condition of allelic inclusion. Immunity *6*, 225–233.

Su, I.H., Basavaraj, A., Krutchinsky, A.N., Hobert, O., Ullrich, A., Chait, B.T., and Tarakhovsky, A. (2003). Ezh2 controls B cell development through histone H3 methylation and Igh rearrangement. Nat. Immunol. *4*, 124–131.

Tavares, L., Dimitrova, E., Oxley, D., Webster, J., Poot, R., Demmers, J., Bezstarosti, K., Taylor, S., Ura, H., Koide, H., et al. (2012). RYBP-PRC1 complexes mediate H2A ubiquitylation at polycomb target sites independently of PRC2 and H3K27me3. Cell *148*, 664–678.

Ui, A., Nagaura, Y., and Yasui, A. (2015). Transcriptional elongation factor ENL phosphorylated by ATM recruits polycomb and switches off transcription for DSB repair. Mol. Cell *58*, 468–482.

van der Lugt, N.M., Domen, J., Linders, K., van Roon, M., Robanus-Maandag, E., te Riele, H., van der Valk, M., Deschamps, J., Sofroniew, M., van Lohuizen, M., et al. (1994). Posterior transformation, neurological abnormalities, and severe hematopoietic defects in mice with a targeted deletion of the bmi-1 proto-oncogene. Genes Dev. *8*, 757–769.

Yancopoulos, G.D., and Alt, F.W. (1985). Developmentally controlled and tissue-specific expression of unrearranged VH gene segments. Cell *40*, 271–281.

Yong, K.J., Basseres, D.S., Welner, R.S., Zhang, W.C., Yang, H., Yan, B., Alberich-Jorda, M., Zhang, J., de Figueiredo-Pontes, L.L., Battelli, C., et al. (2016). Targeted BMI1 inhibition impairs tumor growth in lung adenocarcinomas with low CEBPα expression. Sci. Transl. Med. *8*, 350ra104.

STAR★METHODS

KEY RESOURCES TABLE

REAGENT or RESOURCE	SOURCE	IDENTIFIER
Antibodies		
Rat anti-mouse B220 – APCCy7 (clone: RA3-6B2)	Biolegend	Cat#103223; RRID: AB_313006
Rat anti-mouse CD19 – Pacific Blue (clone: 6D5)	Biolegend	Cat#115526; RRID: AB_493341
Rat anti-mouse ckit – APC (clone: 2B8)	Biolegend	Cat#105805; RRID: AB_313214
Rat anti-mouse CD25 – PE (clone: PC61)	Biolegend	Cat#102007; RRID: AB_312856
Rat anti-mouse IgM – PECy7 (clone: RMM-1)	Biolegend	Cat#406513; RRID: AB_10640069
Rat anti-mouse IgD – PerCP5.5 (clone: 11-26c.2a)	Biolegend	Cat#405709; RRID: AB_1575115
Rat anti-mouse CD4 – FITC (clone: RM4-5)	Biolegend	Cat#100509; RRID: AB_312712
Rat anti-mouse CD8 – APCCy7 (clone: 53-6.7)	Biolegend	Cat#100713; RRID: AB_312752
Rat anti-mouse B220 – Pacific Blue (clone: RA3-6B2)	Biolegend	Cat#103230; RRID: AB_492877
Rat anti-mouse Gr1 – PE (clone: RB6-8C5)	Biolegend	Cat#108407; RRID: AB_313372
Rat anti-mouse TER119 – PerCP (clone: TER119)	Biolegend	Cat#116225; RRID: AB_893637
Rat anti-mouse CD11b – PECy7 (clone: M1-70)	Biolegend	Cat#101215; RRID: AB_312798
AffiniPure Fab Fragment Goat anti-mouse IgM, μ chain specific – FITC	Jackson ImmunoResearch	Cat#115-097-020; RRID: AB_2338618
IgG from rat serum	Sigma Aldrich	Cat#I4131; RRID: AB_1163627
Bacterial and Virus Strains		
NEB 5-alpha competent *E. coli*	New England Biolabs	Cat#C2987I
Chemicals, Peptides, and Recombinant Proteins		
DAPI	Sigma Aldrich	Cat#32670; CAS#28718-90-3
Critical Commercial Assays		
FITC BrdU Flow Kit	BD Biosciences	Cat#559619; RRID: AB_2617060
FITC Annexin V Apoptosis Detection Kit	Biolegend	Cat#640932
Deposited Data		
Pro-B cell RNA-sequencing data	This paper	GEO: GSE119422
Experimental Models: Organisms/Strains		
Mouse: *Bmi1*$^{+/-}$: FVB.129P2-*Bmi1*^{tm1Brn}/MvlJ	Maarten van Lohuizen (van der Lugt et al., 1994)	JAX: 024584
Mouse: *B1.8*$^{+}$: B6.129P2(C)-*Igh*^{tm2Cgn}/J	Klaus Rajewsky (Sonoda et al., 1997)	JAX: 012642
Mouse: *p53*$^{F/+}$: B6.129P2-*Trp53*^{tm1Brn}/J	The Jackson Laboratory	JAX: 008462
Mouse: *Mx1-cre*: B6.Cg-Tg(Mx1-cre)1Cgn/J	The Jackson Laboratory	JAX: 003556
Mouse: *Bmi1*$^{F/+}$: *Bmi1*$^{tm1.1Lees}$/J	The Jackson Laboratory	JAX: 028572
Mouse: *mb1-cre*: B6.C(Cg)-*Cd79a*$^{tm1(cre)Reth}$/EhobJ	The Jackson Laboratory	JAX: 020505
Oligonucleotides		
mRNA expression RT-PCR primer pairs, see Table S3	This paper	N/A
Primer pairs for analysis of VDJ_H joints, see Table S4	This paper	N/A
Software and Algorithms		
FlowJo	FlowJo, LLC	https://www.flowjo.com
Prism	Graphpad	https://www.graphpad.com
ImageJ	NIH	https://imagej.nih.gov/ij/
NCBI IgBlast	NIH	https://www.ncbi.nlm.nih.gov/igblast/
Other		
Poly(I:C)	InvivoGen	Cat#tlrl-picw
BD Cytofix/Cytoperm	BD Biosciences	Cat#554714

(*Continued on next page*)

Continued

REAGENT or RESOURCE	SOURCE	IDENTIFIER
Zoombie UV Fixable Viability Dye	Biolegend	Cat#423107
Propidium Iodide Staining Solution	BD Biosciences	Cat#556463
M-MLV Reverse Transcriptase	Promega	Cat#M1701
Maxima Reverse Transcriptase	Thermo Scientific	Cat#EP0741
Maxima SYBR Green Master Mix	Thermo Scientific	Cat#K0241
Roche Expand High Fidelity PCR System	Roche	Cat#11732641001
pGEM-T Easy Vector System	Promega	Cat#A1360
RNeasy Micro Kit	QIAGEN	Cat#74004
RNeasy Mini Kit	QIAGEN	Cat#74104
DNAeasy Blood and Tissue Kit	QIAGEN	Cat#69504
SMARTer low-input RNA kit	Clontech	Cat#634938

CONTACT FOR REAGENT AND RESOURCE SHARING

Further information and requests for resources and reagents should be directed to and will be fulfilled by the Lead Contact, Gregory David (Gregory.David@nyulangone.org).

EXPERIMENTAL MODEL AND SUBJECT DETAILS

Mx1-Cre, Bmi1$^{F/+}$, *Mb1-cre*, and *p53*$^{F/+}$ mice were purchased from The Jackson Laboratory and have been described (Hobeika et al., 2006; Kühn et al., 1995; Marino et al., 2000; Maynard et al., 2014). *Bmi1*$^{+/-}$ mice were a kind gift from Maarten van Lohuizen and have been described (van der Lugt et al., 1994). *B1.8i* mice were a kind gift from Klaus Rajewsky and have been described (Sonoda et al., 1997). Animals were housed in specific pathogen-free conditions at the Skirball Animal Facility. Aged matched controls were used for *Bmi1* germline mutant mice whereas littermate controls were used for *Bmi1*$^{F/F}$ *Mb1-cre* mice. Female and male mice were used depending on availability. All mice were analyzed at 4-8 weeks of age. All animal experiments were done in accordance with the guidelines of the NYU School of Medicine Institutional Animal Care and Use Facility.

METHOD DETAILS

Mouse treatment

For induction of Cre-mediated deletion of *loxP*-flanked *p53* alleles in the *Bmi1 p53 Mx1-Cre* animal cohort, poly(I:C) (InvivoGen) was administered by i.p. injection at 5μg kg^{-1} in PBS for 3 injections on alternating days at 3 weeks of age. Animals were analyzed two weeks following the last poly(I:C) injection.

Flow cytometry analysis and cell sorting

Single cell suspensions were derived from bone marrow (femur and tibia of both hind legs), spleen, thymus, and peripheral blood. Red blood cells were lysed with ACK lysis buffer. Cell counts were determined using a cell counter (Beckman Coulter) set to detect nuclei between 3.5uM and 10uM or manually with a hemocytometer. All cells were blocked with purified rat IgG (20ug ml^{-1}) for 15 min on ice prior to antibody staining. The following antibodies were used for analysis (from Biolegend): anti-B220 (RA3-6B2), anti-CD19 (6D5), anti-CD4 (RM4-5), anti-CD8 (53-6.7), anti-CD11b (M1-70), anti-Gr1 (RB6-8C5), anti-TER119 (TER119), anti-CD25 (PC61), anti-IgM (RMM-1), anti-IgD (11-26c.2a), and anti-ckit (2B8). Cells were stained with primary antibodies for 30 min on ice. For intracellular staining of Igμ chain, cells were first stained for surface markers followed by fixation and permeabilization with BD Cytofix/Cytoperm for 30 min at room temperature. Cells were then incubated with an Igμ specific Fab fragment (Jackson ImmunoResearch) for 45 min on ice. PI (1ug ml^{-1}), DAPI (500ng ml^{-1}), 7aad (1ug ml^{-1}), or Zombie fixable dye was added following staining for the exclusion of dead cells. Cells were identified based on the cell-surface phenotypes described in Table S2. Cells were analyzed on a LSRII (BD Biosciences) or sorted on an AriaI or AriaII (BD Biosciences). Data were analyzed with FlowJo software (FlowJo, LLC).

RNA-sequencing

RNA was isolated from FACS purified pro-B cells. RNA was harvested from 2 biological replicates using the RNeasy Micro Kit (QIAGEN). RNA quantification and quality was determined using an Aglient 1200 Bioanalyzer. Strand-specific libraries were prepared using the SMARTer low-input RNA kit. Libraries were sequenced on an Illumina HiSeq2500 using 50bp paired-end reads. Fastq files were aligned to mm9 using TopHat. Differential expression tests were done using the Cuffdiff module of Cufflinks against the Refseq

annotation. We used an FDR < 0.05 as a cutoff for significance. Gene set enrichment analysis was performed using $\log_2$ fold change as metric for ranking genes and 1,000 permutations. Gene sets used in this study were identified from the Molecular Signatures Database (Curated v5.0 and Hallmarks v5.0).

Cell cycle analysis

For cell cycle analysis of pre-B cells, cells were stained for surface markers, fixed and permeabilized with BD Cytofix/Cytoperm for 30 min at room temperature, and incubated with DAPI (10μg ml^{-1}) and RNaseA (50μg ml^{-1}) for 30 min at room temperature. For BrdU incorporation analysis of pre-B cells, mice were i.p. injected with 1mg BrdU and sacrificed 2 hr later. Cells were stained for surface markers and analyzed for BrdU incorporation as described using the BD PharMingen BrdU Flow Kit. Apoptotic cells were detected using the Annexin V Apoptosis Detection Kit (Biolegend) according to the manufacturer's instructions.

RT-qPCR analysis

RNA from sorted cell populations was isolated using the RNeasy Mini Kit (QIAGEN). Prior to reverse transcription, RNA was incubated with DNase I (Promega). RNA was subsequently converted into cDNA using either M-MLV reverse transcriptase (Promega) or Maxima reverse transcriptase (Thermo Scientific) according to the manufacturer's instructions, using an equal mix of oligo dT and random hexamers as primers. Real-time quantitative PCR (RT-qPCR) was performed on a Bio-rad iCycler using Maxima SYBR Green master mix (Thermo Scientific) according to the manufacturer's instructions. No-RT controls were included to ensure no genomic DNA contamination was present. All values were normalized to *Hprt* levels using the ΔCt method. RT-PCR primer pairs are shown in Table S3.

Semiquantitative PCR analysis of VDJ_H joints

Genomic DNA from sorted cell populations was isolated using the DNeasy Blood and Tissue kit (QIAGEN). *Igh* rearrangements were amplified as previously described (Fuxa et al., 2004). Briefly, serial dilutions of genomic DNA were amplified using a forward primer specific to either the D_H, the V_H7183 family, or the V_HJ558 family and a reverse primer specific to J_{H3}. Primers specific to Cμ were used as a loading control. PCRs were run in the linear range and products were run on a 1.25% agarose gel. Primer pairs are shown in Table S4.

Sub-clonal sequencing of VDJ_H joints

Genomic DNA from sorted pro-B cells was isolated using the DNeasy Blood and Tissue kit (QIAGEN). *Igh* rearrangements were amplified using a promiscuous forward primer (MsVHe) (5′-GGGAATTCGAGGTGCAGCTGCAGGAGTCTGG-3′) that binds to genes within all V_H families and a reverse primer specific to J_{H3} (5′-GTCTAGATTCTCACAAGAGTCCGATAG ACCCTGG-3′). A high fidelity polymerase (Roche) was used to minimize point mutations during PCR amplification. The amplified product was run on a 1% agarose gel and the expected band size (~450bp) was excised and purified. The purified DNA product was inserted into the pGEM-T easy vector (Promega) according to the manufacturers instructions. Subcloned DNA was column purified (QIAGEN) and sequenced using T7 primer (Macrogen). VDJ_H sequences were analyzed using the National Center for Biotechnology Information's IgBlast program.

DNA FISH

DNA FISH was performed with the probes BACs CT7-199M11 (3' *Igh*) and CT7-526A21 (5' *Igh*) labeled by nick translation. For each 22x22 mm coverslip, 1 μg of labeled BAC DNA, 10 μg of sheared salmon sperm DNA and 1 μg of Cot-1 (Life Technologies) were precipitated and resuspended in 16 μL of hybridization buffer (50% formamide/20% dextran sulfate/5X denhardt's solution). DNA FISH was carried out as previously described (Chaumeil et al., 2008). Briefly, cells were adhered to poly-L-lysine coated coverslips for 10 min, fixed for 10 min at 22°C with 2% (wt/vol) paraformaldehyde/PBS and permeabilized for 10 min with 0.5% (vol/vol) Triton/PBS. Coverslips were incubated with RNaseA (0.1 mg/ml in PBS, 30 min at 37°C), then re-permeabilized for 10 min at 0°C in 0.7% (vol/vol) Triton X-100 / 0.1 M HCl. Cells were then placed in 50% formamide/2XSSC for 1 hr at 22°C. Coverslips and resuspended probes were then placed at 75°C for 2 min, before probes were applied to coverslips, sealed onto slides with rubber cement, followed by incubation overnight at 37°C. Cells were then washed two times with 50%formamide/2xSSC at 42°C, two times with 2xSSC at 42°C and 1xSSC at 42°C, for 5 min each and were mounted in Prolong Gold (Life Technologies) containing 1.5 μg/ml DAPI.

Confocal microscopy and analysis

DNA FISH was imaged by confocal microscopy on a Leica SP5 AOBS system (Acousto-Optical Beam Splitter). Optical sections separated by 0.3 μm were collected and only cells with signals from both alleles were analyzed using ImageJ software (NIH). For distance measurements in DNA FISH, ImageJ was used to measure the center of mass of each focus and calculate intralocus distances.

QUANTIFICATION AND STATISTICAL ANALYSIS

Statistical analysis was performed using an unpaired Student's two-tailed t test. Differences in the distribution of intralocus distance between the 5' and 3' *Igh* FISH probes was compared using the Kolmogorov-Smirnov test. All experiments were performed in the

number of biological replicates mentioned as n in the figure legends or shown as individual points in figures. N represents individual sequences for pro-B cell subclonal VDJ_H joint sequencing, individual cells for DNA FISH assessing *Igh* contraction, and individual animals for all other experiments. A p value < 0.05 was considered statistically significant. All data were analyzed using GraphPad Prism software.

DATA AND SOFTWARE AVAILABILITY

RNA-sequencing data were deposited at GEO and is available under accession GEO: GSE119422.

Cell Reports, Volume *26*

Supplemental Information

Impaired Expression of Rearranged Immunoglobulin Genes and Premature p53 Activation Block B Cell Development in BMI1 Null Mice

David J. Cantor, Bryan King, Lili Blumenberg, Teresa DiMauro, Iannis Aifantis, Sergei B. Koralov, Jane A. Skok, and Gregory David

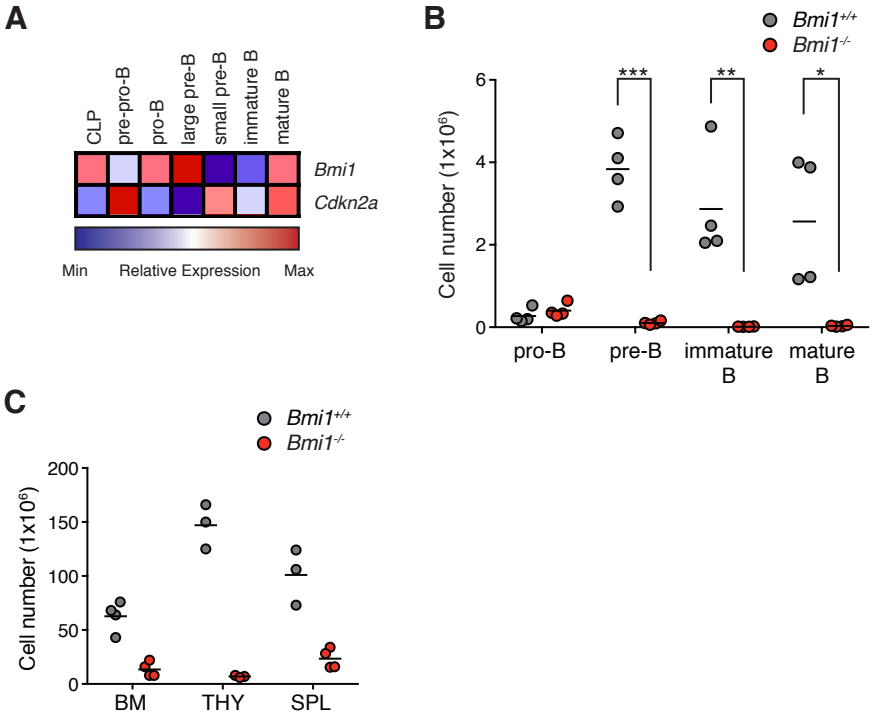

Figure S1, related to Figure 1. BMI1 is highly expressed and functions at the pro-B to pre-B cell transition.

(A) Expression pattern of *Bmi1* and *Cdkn2a* in developing B cells from the Immunological Genome Project (Painter et al., 2011). **(B)** Cell number of developing B cells in the bone marrow of indicated mice. Each point represents one animal; line represents the mean. n=4 for each genotype. **(C)** Cellularity of bone marrow, thymus, and spleen from indicated mice. Each point represents one animal; line represents the mean. $n \geq 3$ for each genotype. ***$p<0.001$, **$p<0.01$, *$p<0.05$. BM: bone marrow. THY: thymus. SPL: spleen.

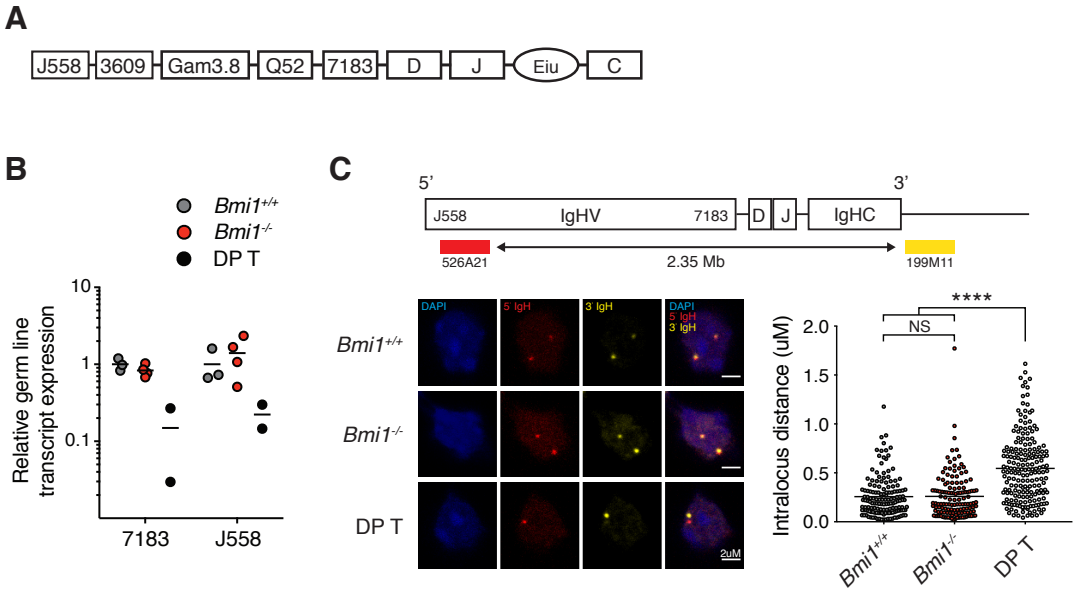

Figure S2, related to Figure 2. BMI1 is not required for *Igh* germ line transcription or *Igh* contraction. **(A)** Diagram of *Igh* locus with distal and proximal VH families indicated. **(B)** RT-qPCR expression analysis of germline transcription of both proximal (7183) and distal (J558) VH gene families from sorted pro-B cells from indicated mice. DP T were used as a negative control. Each point represents one animal; line represents the mean. n=3 for *Bmi1*$^{+/+}$ animals; n=4 for *Bmi1*$^{-/-}$ animals; n=2 for DP T. **(C)** Analysis of *Igh* contraction in pro-B cells using 3-D microscopy with proximal and distal DNA FISH probes as depicted in the diagram. 2.35 Mb separate the two DNA FISH probes. Left: representative images. Scale bars, 2 μM. Right: quantification of intralocus distance. DP T were used as a negative control. 2 independent experiments were done with >100 cells calculated for each genotype. Each point represents one cell; line represents the mean. ****p<0.0001, *p<0.05. NS: not significant. DP T: double positive thymocytes.

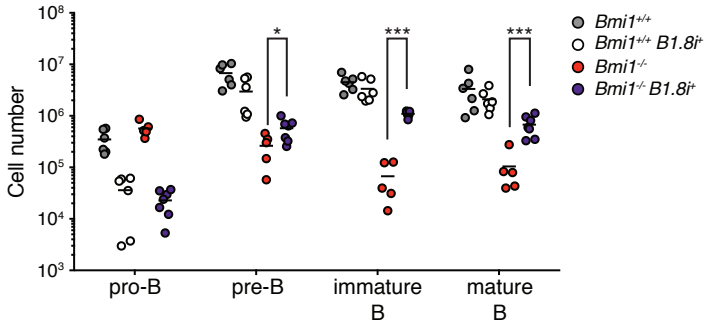

Figure S3, related to Figure 3. Bypassing VDJ_H rearrangement rescues B cell development in *Bmi1*$^{-/-}$ mice.

Cell number of indicated progenitor B cell type in the bone marrow of indicated mice. Each point represents one animal; line represents the mean. $n \geq 5$ for each genotype. ***$p<0.001$, *$p<0.05$.

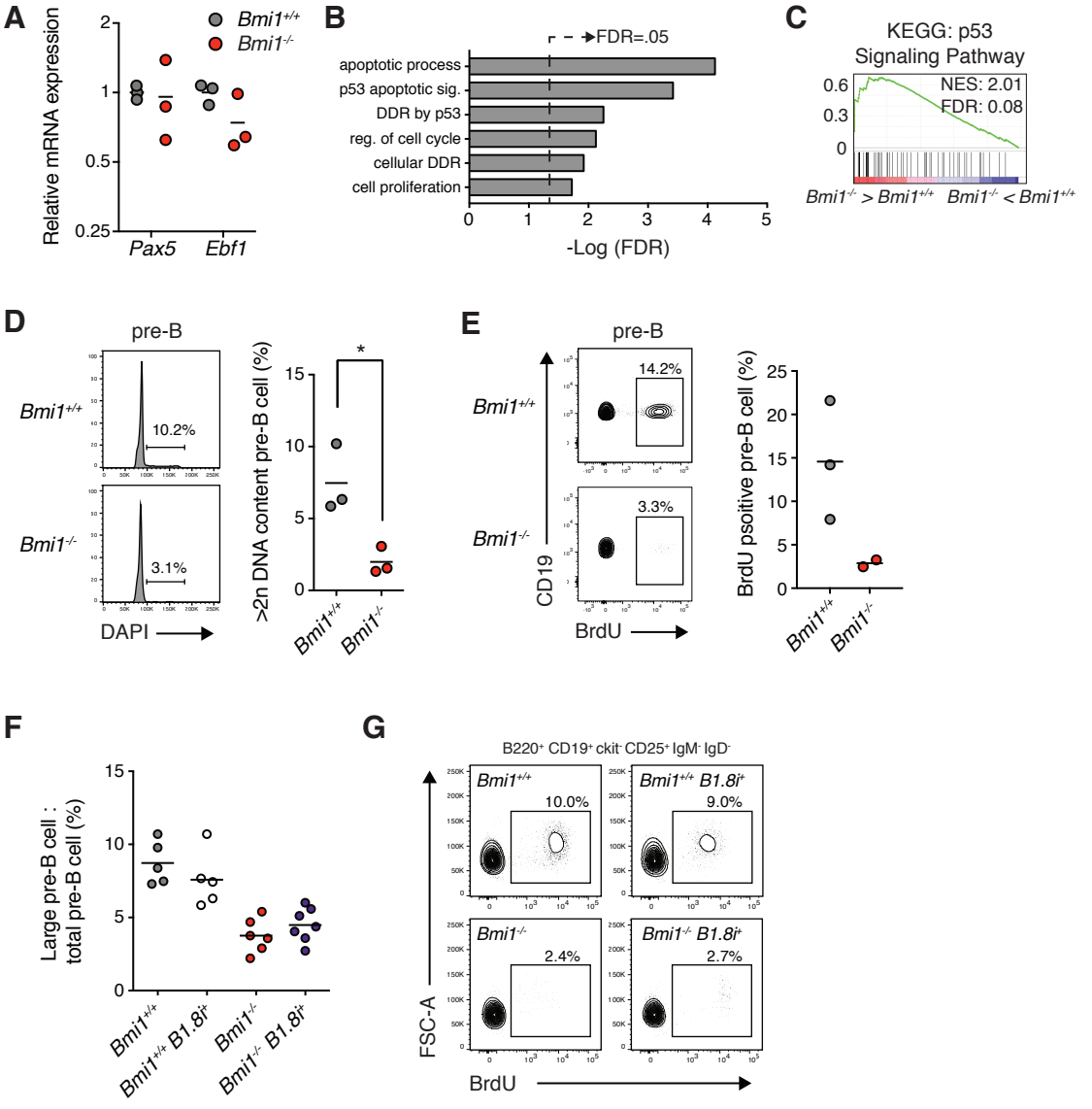

Figure S4, related to Figure 4. BMI1 prevents inappropriate p53 signaling in pro-B cells.
(A) mRNA expression levels as determined by RT-qPCR of indicated genes from pro-B cells of indicated mice. Each point represents one animal; line represents the mean. n=3 for each genotype. **(B)** Gene ontology analysis of upregulated genes in *Bmi1*$^{-/-}$ pro-B cells. **(C)** Gene set enrichment analysis identified that the p53 signaling pathway is enriched in *Bmi1*$^{-/-}$ pro-B cells. **(D)** Representative FACS plot and frequency of pre-B cells that have >2n DNA content (cells in S-G2-M phases of cell cycle) in indicated mice. Each point represents one animal; line represents the mean. n=3 for each genotype. **(E)** Representative FACS plot and frequency of BrdU^{+} pre-B cells in indicated mice. Animals received an i.p. injection of 1mg BrdU and were analyzed two hours later. Each point represents one animal; line represents the mean. n=3 for *Bmi1*$^{+/+}$ animals; n=2 for *Bmi1*$^{-/-}$ animals. **(F)** The frequency of large pre-B cells present in the pre-B cell compartment of indicated mice. Each point represents one animal; line represents the mean. n ≥ 5 for each genotype. **(G)** FACS plot of BrdU^{+} pre-B cells in indicated animals. Animals received an i.p. injection of 1mg BrdU and were analyzed two hours later. *p<0.05.

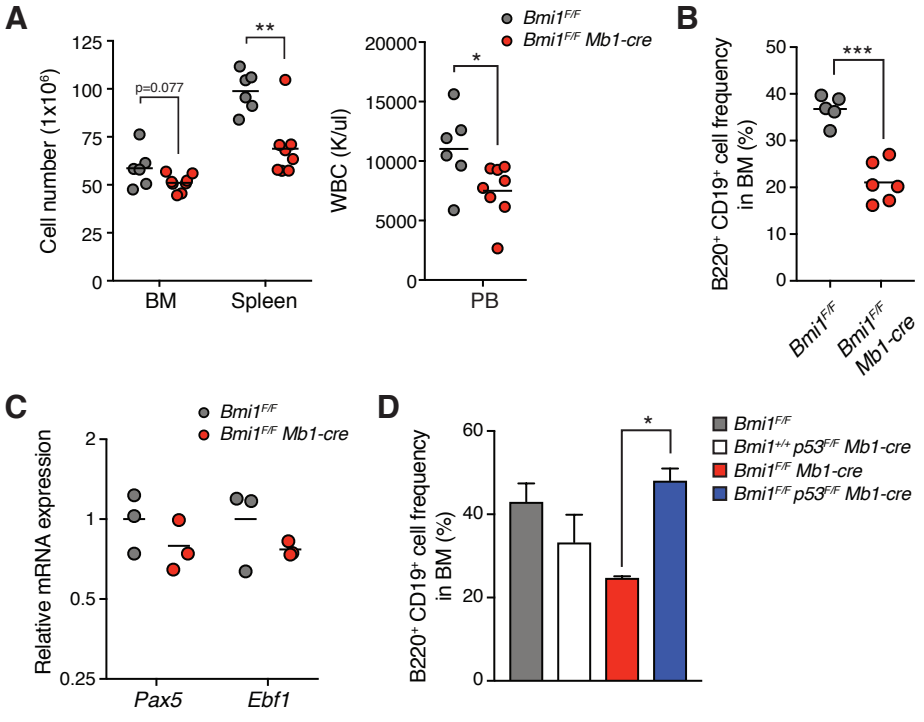

Figure S5, related to Figure 5. BMI1 functions in a cell autonomous manner to regulate B cell development. **(A)** Cell number in the spleen, bone marrow, and peripheral blood of indicated mice. Each point represents one animal; line represents the mean. n=6 for *Bmi1*$^{F/F}$ animals; n=8 for *Bmi1*$^{F/F}$ *Mb1-cre* animals. **(B)** Frequency of B220^{+} CD19^{+} cells in the bone marrow of indicated mice. Each point represents one animal; line represents the mean. n=5 for *Bmi1*$^{F/F}$ animals; n=6 for *Bmi1*$^{F/F}$ *Mb1-cre* animals. **(C)** mRNA expression levels as determined by RT-qPCR of indicated genes from pro-B cells of indicated mice. Each point represents one animal; line represents the mean. n=3 for each genotype. **(D)** Frequency of B220^{+} CD19^{+} cells in the bone marrow of indicated mice. Data represents mean ± sem. n=3 for each genotype. ***p<0.001, **p<0.01, *p<0.05. BM: bone marrow. PB: peripheral blood. WBC: white blood cell.

Cell Population	Cell-surface phenotypes
Pro-B	$B220^{+}$ $CD19^{+}$ $ckit^{+}$ $CD25^{-}$ IgM^{-} IgD^{-}
Pre-B	$B220^{+}$ $CD19^{+}$ $ckit^{-}$ $CD25^{+}$ IgM^{-} IgD^{-}
Large Pre-B	$B220^{+}$ $CD19^{+}$ $ckit^{-}$ $CD25^{+}$ IgM^{-} IgD^{-} FSC^{high}
Small Pre-B	$B220^{+}$ $CD19^{+}$ $ckit^{-}$ $CD25^{+}$ IgM^{-} IgD^{-} FSC^{low}
Immature B	$B220^{+}$ $CD19^{+}$ IgM^{+} IgD^{-}
Mature (recirculating) B	$B220^{+}$ $CD19^{+}$ IgM^{+} IgD^{+}
DP Thymocytes	Lin (B220, TER119, Gr1, CD11b)$^{-}$ $CD4^{+}$ $CD8^{+}$

Table S2, related to STAR methods. Flow cytometry cell surface phenotypes.

Gene	5’ oligo	3’ oligo
Hprt	AGG TTG CAA GCT TGC TGG T	TGA AGT ACT CAT TAT AGT CAA GGG CA
Bmi1	TGC AGA TGA GGA GAA GAG GA	TCA TTC ACC TCT TCC TTA GGC
p19^{Arf}	GCT CTG GCT TTC GTG AAC ATG	TCG AAT CTG GAC CGT AGT TGA G
Bbc3	CTG GAG GGT CAT GTA CAA TCT C	GGT GTC AGA AGG CGG AG
Pmapi1	CGG ACA TAA CTG TGG TTC TGG	ACA CTC GTC CTT CAA GTC TGC
Bax	AAA CTG GTG CTC AAG GCC C	CTT GGA TCC AGA CAA GCA GC
Phlda3	AGA CAT GTC AGC TTC TCT GTC C	CTA CTG GCT TCT GCT CTC CG
C*dkn1a*	AGA GAC AAC GGC ACA CTT TG	CAG ACA TTC AGA GC CACA GG
Trp53	TGA ACC GCC GAC CTA TCC TTA CC	CCC AGG GCA GGC ACA AAC AC
Pax5	GGA CCA TCA GGA CAG GAC AT	ACA GCA ATG GGA TAC GGA CA
Ebf1	ACA GCA ATG GGA TAC GGA CA	CGT GTG TGA GCA ATA CTC GG
D_H-Cμ	TTC AAA GCA CAA TGC CTG GCT	ATG CAG ATC TCT GTT TTT GCC TCC
V_H7183-Cμ	CGG TAC CAA GAA SAM CCT GTW CCT GCA AAT GAS C	ATG CAG ATC TCT GTT TTT GCC TCC
V_HQ52-Cμ	CGG TAC CAG ACT GAR CAT CAS CAA GGA CAA YTC	ATG CAG ATC TCT GTT TTT GCC TCC
V_HGam3.8-Cμ	CAA GGG ACG GTT TGC CTT CTC TTT GGA A	ATG CAG ATC TCT GTT TTT GCC TCC
V_H3609-Cμ	KCY YTG AAG AGC CRR CTC ACA ATC TCC	ATG CAG ATC TCT GTT TTT GCC TCC
V_HJ558-Cμ	CGA GCT CTC CAR CACA GC CTW CAT GCA RCT CAR C	ATG CAG ATC TCT GTT TTT GCC TCC
V_H7183 GLT	GCC TCT GGA TTC ACT TTC AG	CAT TGT CTC TGG AGA TGG TG
V_HJ558 GLT	CTT CTG GCT ACA CCT TCA C	CTG AGC TGC ATG TAG GCT G

K: G,T M: A,C R: A,G S: C,G W: A,T Y: C,T

Table S3, related to STAR methods. mRNA expression RT-qPCR primer pairs.

DNA product	**5' oligo**	**3' oligo**
$D_H - J_{H3}$	TTC AAA GCA CAA TGC CTG GCT	GTC TAG ATT CTC ACA AGA GTC CGA TAG ACC CTG G
$V_H7183 - J_{H3}$	CGG TAC CAA GAA SAM CCT GTW CCT GCA AAT GAS C	GTC TAG ATT CTC ACA AGA GTC CGA TAG ACC CTG G
$V_HJ558 - J_{H3}$	CGA GCT CTC CAR CACA GC CTW CAT GCA RCT CAR C	GTC TAG ATT CTC ACA AGA GTC CGA TAG ACC CTG G
Cμ	TGG CCA TGG GCT GCC TAG CCC GGG ACT T	GCC TGA CTG AGC TCA CAC AAG GAG GA
MsVHe - J_{H3}	GGG AAT TCG AGG TGC AGC TGC AGG AGT CTG G	GTC TAG ATT CTC ACA AGA GTC CGA TAG ACC CTG G

R: A,G S: C,G W: A,T

Table S4, related to STAR methods. Primer pairs for analysis of *VDJ_H* joints.